Sudan University of Science and Technology

College of graduates study

Department of Biomedical Engineering

DESIGN AND IMPLEMENTATION OF NON-INVASIVE MALARIA DETECTION SYSTEM

Submitted in partial fulfillment of the requirement of

M.Sc (honor) Degree in Biomedical Engineering

SUBMITTED BY:

Tawasul Adil Hussein Ali

SUPERVISED BY:

DR. *Magdi Bakr*

January 2015

Dedication

To…

MY LOVELY BELOVED FATHER

To …

MY SWEETEST BELOVED MOTHER

I DEDICATE THIS RESEARCH

‘‘‘‘

Acknowledgements

All thanks to Allah Almighty who gave me the strength, Determination, health and granted me with patience to successfully complete of this research.

I cannot express enough thanks to my supervisor **Dr. Magdi Baker Amen** for his continued guidance, support, unlimited helps and encouragement; I offer my sincere appreciation for the learning opportunities provided by you.

My completion of this research could not have been accomplished without the support of my **parents**. My deepest gratitude, special appreciation and thanks to: Biomedical Engineering department staff, Mechanical Engineering school staff specially **DR. Yassin Hamdan** who guide me to complete my mechanical design, Sudanese Germany laboratory centre, **Eng. Ayman Kenana**, **Eng. Rayan Mergani**, and my friend **Eng. Olla Salahaldin** for their support and guidance. Your encouragement when the times got rough are much appreciated and duly noted.

Contents

Chapter three :Theoretical background

Chapter four: design and implementation

List of Tables

List of figures

ABBREVIATIONS

Ampere	A
Analog to Digital Converter	ADC
Artificial Neural Networks	ANNs
Advance Virtual Risk	AVR
Deoxyribose-Nucleic Acid	DNA
Degree	^{o}
Enzyme-Linked Immunosorbent Assay	ELISA
Ground	GND
Hertz	Hz
Infra-Red	IR
Light Amplification by Stimulated Emission of Radiation	LASER
Liquid Crystal Display	LCD
Millimeter	mm
Millivolt	mV
Magneto-Optical Technique	MOT
Polymerase Chain Reaction	PCR
Plasmodium Falciparum	P. F
Plasmodium Malariae	P.M
Plasmodium Ovale	P.O
Plasmodium Vivax	P.V
Scatter angle	Sc
Rapid Detection Test	RDT
Tesla	T
World Health Organization	WHO
Ohm	Ω

Abstract

This research focuses on quantify presence of malaria pigment (hemozoin) in blood stream by measuring the two properties of light interaction with hemozoin crystal: scatter angle and absorption of laser infrared when interacting with hemozoin particles on application of a magnetic field and pressure force in a non-invasive way. The prototype contains Laser infrared source, permanent magnet and embedded system (SOC) in-order to diagnose malaria type and prove the relationship between infrared scatter angle, absorption, and hemozoin presence. And combine between two results to find the best non invasive way which present better result than other method used.

Fifty two total cases taken from Sudanese Germany centre laboratory divided into two parts: thirty two positive and twenty negative readings had been tested with the prototype which gives test accuracy of (**90.38** %)and sensitivity percentage (**93.7** %), with combining results of scatter angle 5^{o} and absorption value between (290 mV to 449 mV) for **malarial cases**, (2^{o} to 4^{o}) and (450mV to 1248mV) for **non-malarial cases** .

Non-invasive, less pain and more comfortable malaria test was presented at small area with high performance and small duration (50 sec\person), by this study.

المستخلص

يركز هذا البحث على تحديد وجود صبغة الملاريا (هيموزوين) في مجرى الدم دون حقن عن طريق قياس اثنين من خصائص الضوء عند تفاعله مع هذه الصبغة :زاوية التشتت والامتصاص باستخدام مصدر ليزر للأشعة تحت الحمراء وتطبيق مجال مغناطيسي مع ضغط مساوي للجسم بعدها يتم تجميع هذه القراءات والعمل على تكبيرها باستخدام مكبر العمليات وفلترتها لتصبح جاهزة لمعالجتها باستخدام المعالج الدقيق واظهار النتائج في شاشة القراءة وذلك من أجل تشخيص نوع الملاريا وإثبات العلاقة بين الأشعة تحت الحمراء وزاوية التشتت، الامتصاص، ووجود هيموزوين .والجمع بين النتيجتين لإعطاء النتيجة النهائية للفحص.

إثنان وخمسون مجموع الحالات التي اتخذت من مختبر المركز السوداني الألماني بعد فحصها قسمت إلى قسمين :(32) حالة ملاريا وعشرون نتيجة سلبية للفحص وتم اختبارها بواسطة النموذج المقترح الذي أعطي نتائج بقراءات: زاوية التشتت 5 درجات والأمتصاص في الحدود من 290 ملي فولت إلى 449 ملي فولت (**(لحالات وجود الملاريا)** و نتائج قراءات: زاوية التشتت من (1 الى 4) درجات والأمتصاص في الحدود من 450 ملي فولت إلى 1249 ملي فولت **(لحالات عدم وجود الملاريا)** بدقة اختبار **90.38**٪ ونسبة حساسية **93.7**٪للجهاز.

هذه الطريقة اعطت اختبار لمرض الملاريا بدون ألم براحة أكثر في مع قدرة أداء عالية وفترة زمنية صغيرة (50)ثانية/للشخص.

Chapter One

Introduction

1.1 Background

Malaria is a life-threatening disease caused by parasites that are transmitted to people through the bites of infected mosquitoes; this parasite lives part of its life in humans and part in mosquitoes. Malaria remains one of the major killers of humans worldwide, threatening the lives of more than one third of the world's population. It thrives in the tropical areas of Asia, Africa, and Central and South America, where it strikes millions of people. Each year 350 to 500 million cases of malaria occur worldwide. Sadly, more than 1 million of its victims, mostly young children, die yearly. [1]

According to the World malaria report (2013), there were (216) million cases of malaria and an estimated (655,000) deaths in (2012). Malaria mortality rates have fallen by more than (25%) globally since (2000), and by (33%) in the WHO African Region. Most deaths occur among children living in Africa where a child dies every minute of malaria and the disease accounts for approximately (22%) of all childhood deaths [2].

1.2 Spread of Malaria

Many biological and environmental factors shape the character of malaria in a given location. Nearly all the people who live in endemic areas are exposed to infection repeatedly. Those who survive malaria in childhood gradually build up some immunity. They may carry the infection, serving as reservoirs for transmission by mosquitoes without developing severe disease. In other areas, where the infection rate is low, people do not develop immunity because they rarely are exposed to the disease. This makes them more susceptible to the ravages

of an epidemic. An epidemic can occur when conditions, such as those discussed below, allow the mosquito population to increase suddenly [2].

Figure (1.1): The global distribution of malaria. [2]

1.3 Overviews of literature reviews

Reviews of the current methodology and approaches to diagnosis of malaria give many advantages of some methods in addition to a few disadvantages may give a mistake or wrong results, the golden smear (conventional light microscopy) is top way to diagnose malaria unfortunately it depends directly on laboratory technicians skills.

Other techniques use a Fluorescent dyes to view parasites at DNA and RNA but although it fairly quick and easy to use, it limited performance when other species of Plasmodium more than falciparum involved and in parasitemia determination (quantification of relative content of parasites in the blood) [6].

In addition to other techniques review in chapter (2) that describes their method, advantages and disadvantages; that generate problem statement of this research.

1.4 Problem Statement

Malaria is a serious disease whose confirmation in laboratories. Some methods which use in malaria detection are time consuming, complex and depend mainly on the skill base of laboratory technicians, while others are too costly and limited in detecting type of malaria.

1.5 **Objectives**

The general objective of this project is to prove a novel technique for detecting malaria and classifying its types non-invasively using magneto-optical technique (MOT).

The specific objective is to:

1. Design a completely non-invasive prototype requiring no blood sample.
2. Detect malaria parasite depending on the scattering angle and absorption of laser infrared applied to the hemozoin molecule which is the waste product of malaria parasite (when it invade the hemoglobin).
3. Examine the distribution of parasite components in an infected red blood cell using magneto-optical technique (MOT) and compare it without using magnet.
4. Evaluate the performance of the developed model results compared to conventional light microscopy (laboratories results).
5. Achieve low cost and less pain high performance with small duration.

1.6 Significance of the Study

Malaria remains a serious worldwide health concern that detected with a regular conventional light microscopy by taking a painful blood sample from patient. For this reason, there is need for quick, painless and accurate diagnosis of malaria. . Non invasive detection of malaria parasites has the potential of replacing a trained

human eye with a trained vision instrument. This will result in Achieve low cost, less pain, high performance speed and accuracy in malaria diagnostics translating to effective management of the disease.

1.7 Hemozoin crystal specifications

Hemozoin is a toxic substance that excretes from malaria parasite, hemezoin production and specifications specially magneto optical (Ferro material magnetizing, absorption and scattering) descriptions will be represented at this section.

1.7.1 Hemozoin Production

During infection, malarial parasites invade erythrocytes and digest the protein (globin) part of the hemoglobin molecule. The heme component, which is toxic to the parasite, is converted into insoluble hemozoin in the form of rodlike crystals; the transformation of low-spin (Fe^{+2}) diamagnetic oxyhemoglobin into high-spin (Fe^{+3}) paramagnetic hemozoin produces a change in magnetic state of blood [4]. Initially hemozoin is deposited in vacuoles within the erythrocytes, and then it's released into suspension in the plasma on rupture of the parasitized erythrocytes, from where it is ultimately scavenged by leukocytes.

On application of a magnetic field, the paramagnetic crystals will become weak bar magnets experiencing a torque seeking to orient them along the applied field direction [4, 7], as show in figure (1.6).

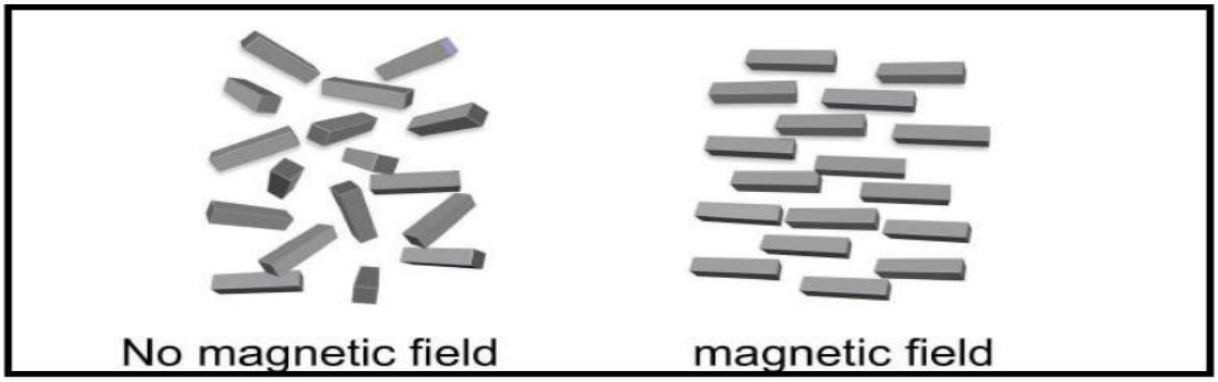

Figure (1.2):Hemozoin molecular before and after application of magnetic field.[5]

1.7.2 Crystal substance Optical specifications

The interaction of light with tissue in the near infrared region can mainly be characterized by two phenomena: absorption and scattering. The distinction between absorption and scattering is not always clear cut but fortunately it has wide differences with hemezoin crystal. Here absorption is defined as the processes where the energy of a light photon is taken up by a molecule without the re-emission of another photon (assuming that one ignores the thermal photons resulting from the heating caused by the energy absorption). Scattering is defined as the processes where the initial direction of a photon changes due to an interaction with a scattering object.

1.8 Thesis layout

This research was divided into six chapters:

Chapter one: Introduction that includes background and spread of malaria, problem statement, objectives…etc.

Chapter two: Literature reviews malaria history, invasive and non invasive malaria diagnosis).

Chapter three: Theoretical Background (light interaction with human body, scattering and absorption theories).

Chapter four: Design and Implementation which contained methodology block diagram, calculations of model, design and implementation of model.

Chapter five: Result and Discussion which discuss an output results and compare it with laboratory results.

Chapter six: Conclusion and Recommendations of the research.

Chapter two

Literature reviews of malaria

This chapter reviews five parts: malaria history: (causes, symptoms, the life cycle and stages of Plasmodium are presented followed by type of malaria), invasive diagnosis of malaria, non invasive malaria detection methods, body anatomy and its interaction with electromagnetic wavelength**.**

Diagnosis of malaria ranges from the labour intensive routine laboratory examination of stained blood smears (films) in light to sophisticated spectroscopic analysis of blood components or application of advanced molecular biology techniques such as Polymerase Chain Reaction (PCR) procedures. Application of digital image processing to the malaria diagnostics problem and the utility of multispectral imaging to myriad applications involving parasite detection and MOT diagnostics are also reviewed.

2.1 **Cause of Malaria**

Malaria is caused by a single-celled parasite from the genus Plasmodium; they produce malaria in many types of animals and birds, as well as in humans. Alphonse Laveran discovered the real cause of malaria, the single-celled Plasmodium parasite. Almost 20 years later, scientists working in India and Italy discovered that Anopheles mosquitoes are responsible for transmitting malaria. [7]

2.1.2 Plasmodium Life cycle

Malaria is a disease caused by a single-celled parasite that lives part of its life in humans and part in mosquitoes. Infection in humans begins when the infected female anopheles mosquito injects the sporozoite parasitic form from its salivary glands into the bloodstream during a blood meal. The sporozoites are carried to the liver, where they undergo asexual production .When these infected liver cells

burst, merozoites are released into the blood, where they invade red blood cells. The intraerythrocytic parasite develops through ring forms into schizonts that produce more infectious merozoites that affect additional red cells [25].

The periodic fever is the result of synchronization of red cell lysis and release of more merozoites. Some of the organisms develop into distinct sexual forms (gametocytes) which, if ingested by the Anopheles mosquito during a feeding, can undergo sexual reproduction that starts the cycle over again [25].

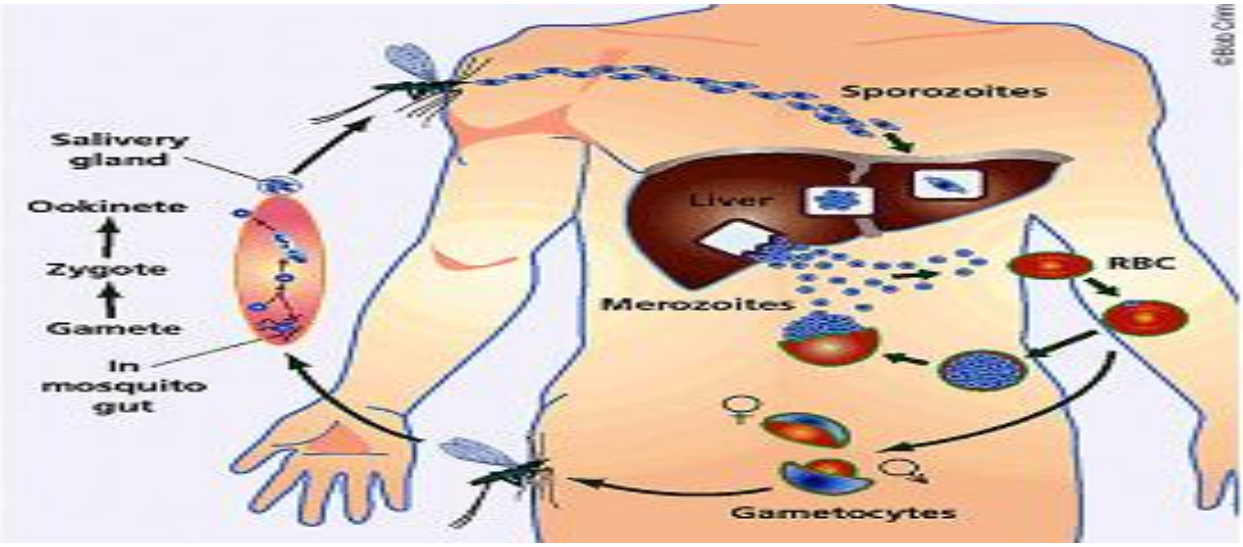

Figure (2.1): Plasmodium life cycle [31].

2.1.3 Malaria types

Infections in humans are caused by four different species of the genus Plasmodium [25]:

- Plasmodium falciparum.
- Plasmodium malariae.
- Plasmodium vivax.
- Plasmodium ovale.

Plasmodium falciparum: is responsible for most malaria deaths, especially in Africa. The infection can develop suddenly and produce several life-threatening

complications. With prompt, effective treatment, however, it is almost always curable [7].

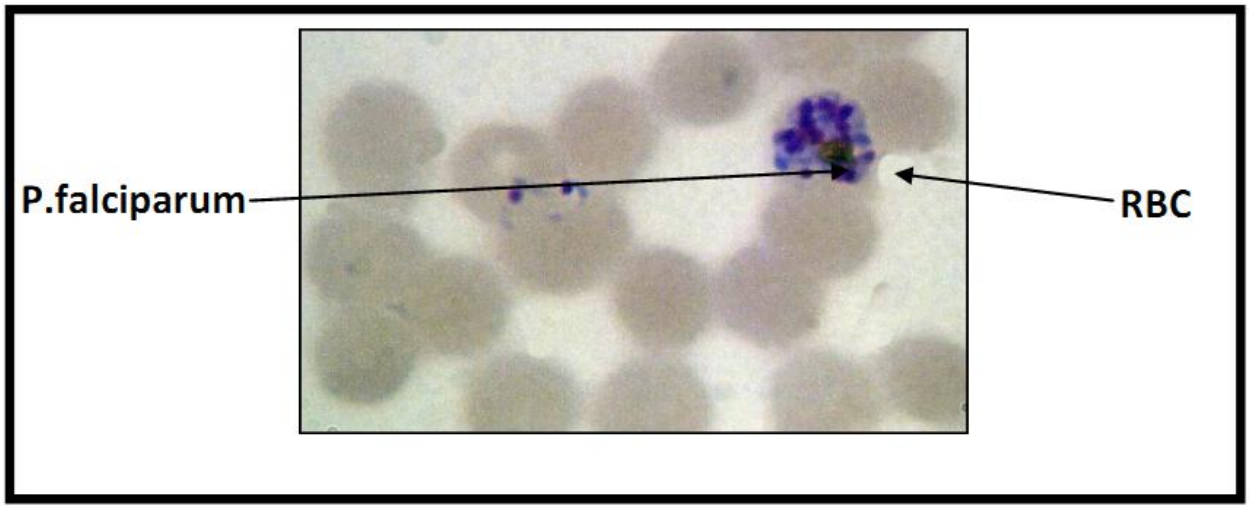

Figure (2.2): Malaria parasite species (P.F) [32].

Plasmodium vivax: is the most geographically widespread of the species produces less severe symptoms. Relapses, however, can occur for up to (3) years and chronic disease is debilitating. Once common in temperate climates, P.vivax is now found mostly in the tropics, especially throughout Asia [1].

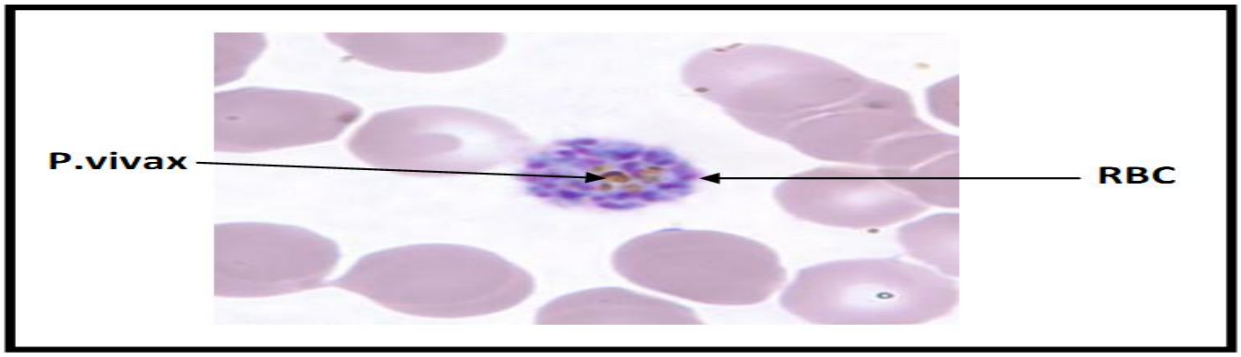

Figure (2.3): Malaria parasite species (P.V) [33].

Plasmodium malariae infections: is not only produce typical malaria symptoms but also can persist in the blood for very long periods, possibly decades, without ever producing symptoms. A person with asymptomatic (no symptoms) P. malariae,

however, can infect others, either through blood donation or mosquito bites. P. malariae has been wiped out from temperate climates, but it persists in Africa [3].

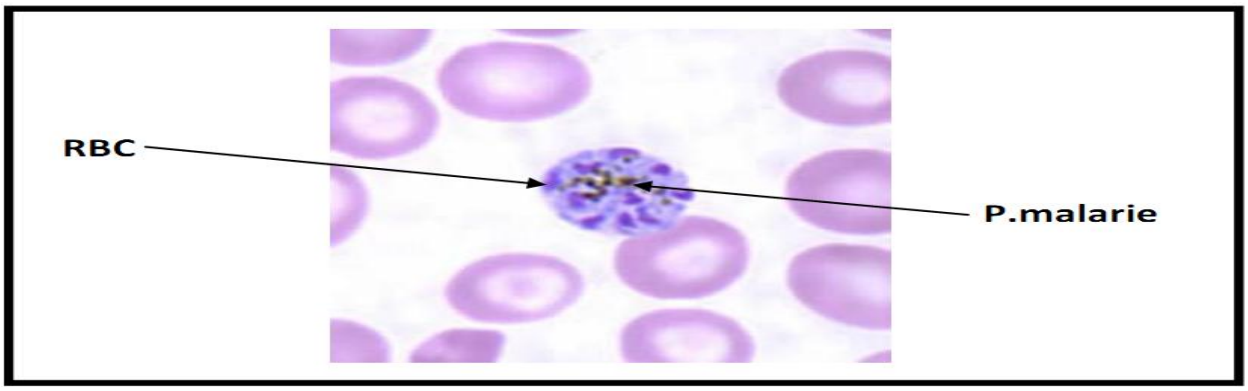

Figure (2.4): Malaria parasite species (P.M) [34]

Plasmodium oval is rare, can cause relapses, and generally occurs in West Africa [7].

Plasmodium falciparum and Plasmodium vivax are the most common; Plasmodium falciparum is the most deadly.

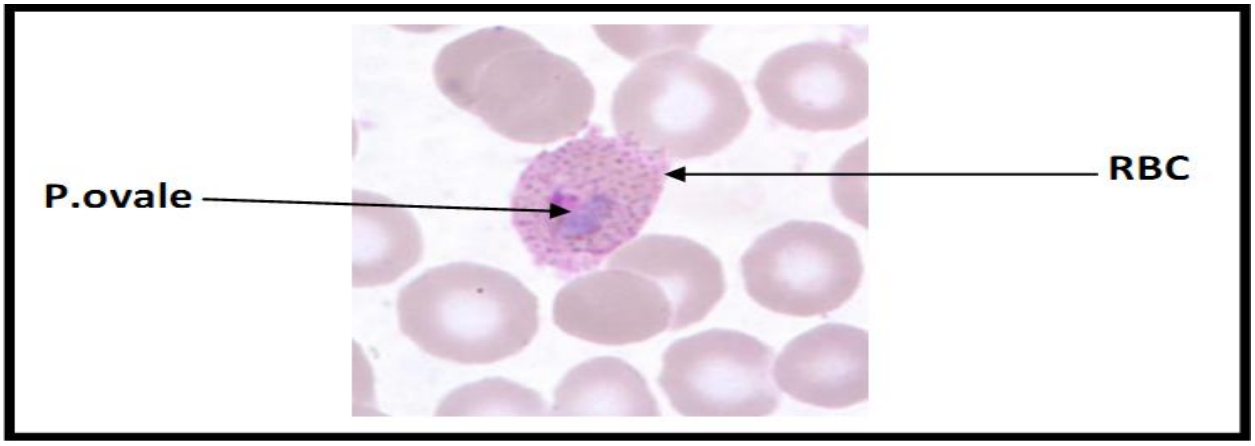

Figure (2.5): Malaria parasite species (P.O) [35].

2.2 Methods for malaria diagnosis

There are different diagnostic methods, the most common are invasive such as Conventional Microscopy and Dark-field microscopy, and some are noninvasive such as Third Harmonic Generation (THG) imaging spectroscopy and UV-visible spectroscopy, and they will be reviewed in section 2.2.1 and 2.2.2.

2.2.1 Invasive malaria diagnosis techniques

Dr. R.K.Srivastava, Laboratory diagnosis of malaria, Ministry of health, 2006. Examined of stained blood film under a conventional light microscope is currently the "gold standard" for laboratory confirmation of malaria. Peripheral blood from a finger (or the heel in young infants) is smeared on a glass slide, stained and fixed (for thin blood smear) to highlight the malaria parasites. Giemsa staining is the most commonly used method and allows identification of all the four species of Plasmodia, stage and parasitemia (relative quantity of parasites in blood) [7] with thin and thick smear [8].

The aforementioned limitations experienced in conventional light microscopy have stimulated research in development of alternative diagnostic methods that could be rapid, sensitive and affordable. Optical enhancement techniques such as dark field microscopy can be employed to significantly reduce the time spent on parasite staining in conventional transmission light microscopy.

Jamjoom [28] used dark-field microscopy to detect presence of malaria parasites in unstained blood films, and observed that intra-erythrocytic stages of Plasmodium (rings, trophozoites and schizonts) and gametocytes were visible as bright objects enclosed in red blood cell outlines against a dark background. This observation

may be understood in terms of Huygen's principle that "If a wave-front strikes an interface between materials with different refractive indices at angle different from 90^{o}, every point of the interface becomes a source of spherical waves". However, identification of the various stages of the parasites was difficult and, like in conventional light microscopy, the method is tedious due to manual examination.

Although microscope consider the gold standard method in malaria diagnose it has some deficiency, High quality malaria microscopy is costly and not always immediately available in every clinical setting where patients might seek medical attention, also this test depend mainly on the skill base of laboratory technicians.

Fluorescent dyes such as acridine orange and benzothiocarboxypurine are nucleic acid selective fluorescent cationic dyes that can bind on DNA and RNA of a biological cell in a process known as electrophoresis [11]. The compound formed fluoresces in the visible region when excited by UV light of appropriate wavelength, hence nucleic acid-containing cells such as malaria parasites are highlighted in a blood smear. A microhaematocrit tube containing acridine orange stain and an anticoagulant is filled with a suspected malaria infected blood obtained by the conventional finger pricking method [12].

Although fluorescent-based techniques are fairly quick and easy to use, they have limited performance when other species of Plasmodium other than falciparum are involved and in parasitemia determination (quantification of relative content of parasites in the blood). These limitations pertain to the fact that the morphology of the parasites is not apparent when fluorescent dyes are used to highlight the parasites [13].

Immunochromatography relies on the migration of liquid across the surface of a nitrocellulose membrane. Immunochromatographic test (commercially presented as Rapid Diagnostic Test kits) are based on the capture of parasite antigen from human blood using monoclonal antibodies prepared against a malaria antigen target and conjugated to a visually detectable marker such as selenium dye or colloidal gold in a mobile phase. Marcucci C, Madjdpour C, Spahn D, Allogeneic blood transfusions: benefit, risks and clinical indications in countries with a low or high human development index, 2004. This study show that RDT tests are based on the detection of antigen(s) released from parasitized red cells. Malaria antigens currently targeted by rapid diagnostic tests (RDT) are histidine-rich proteins 2 (HRP-2), Plasmodium lactate dehydrogenase (PLDH) and Plasmodium aldolase [14]. Dr summiya nizamuddin, Antimicrobial Resistance Network, 2009. This assay explain that RDTs are lateral flow 'immuno-chromatographic' antigen-detection tests, which rely on the capture of dye-labeled antibodies to produce a visible band on a strip of nitro-cellulose .

The problems of this method are that the use of the RDT does not eliminate the need for malaria microscopy. The RDT may not be able to detect some infections with lower numbers of malaria parasites circulating in the patient's bloodstream. Also, there is insufficient data available to determine the ability of this test to detect the two less common species of malaria, P. ovale and P. malariae.

Polymerase Chain Reaction (PCR) is a technique in molecular biology that is used to target and amplify any specific nucleic acid from a complex biological sample. In disease diagnostics, the procedure is used to determine whether a clinical sample contains nucleic acid sequence that is known to occur only in a specific pathogen. The method relies on thermal cycling, consisting of cycles of repeated heating and cooling of the reaction for DNA melting and enzymatic replication of the DNA.

The major advantages of using PCR-based technique are the ability to detect malaria parasites in patients with low levels of parasitemia and to identify them to the species level. Infections with five parasites or less per micro-liters of blood can be detected with 100 % sensitivity and equal specificity [15, 16]. However, PCR-based techniques remain unutilized because they are time-consuming, involve complicated procedures and require a well established laboratory.

2.2.2 Non invasive malaria diagnosis techniques

Spectroscopic techniques such as Third Harmonic Generation (THG) imaging spectroscopy [17], resonance Raman micro-spectroscopy [18,19], and Electron Paramagnetic Resonance (EPR) spectroscopy [20] among others have been used in the investigation of malaria pigment (hemozoin) in malaria drug-target interaction research and in malaria diagnostics studies. Ong et al. [18] Employed resonance Raman micro spectroscopy to study normal and Plasmodium berghei-infected mouse erythrocytes. They found that the Raman spectra for infected and non-infected red blood cells could be differentiated by the bands at 754 cm^{-1} and 747 cm^{-1} respectively. They attributed the slight decrease in frequency between 754 cm^{-1} and 747 cm^{-1} as a result of infection to the fact that, in hemozoin (a polymer formed as a result of haemoglobin degradation by malaria parasites), the porphyrin structures are more packed, resulting in stronger vibrational mode than in haemoglobin.

They also observed that the averaged Raman spectra of infected erythrocytes were identical to Raman spectra of β-hematin (a synthetic analog of hemozoin), implying that hemozoin was indeed the spectroscopic biomarker of Plasmodium infection.

Belislie et al. [17] developed an optical based malaria detection method using Third Harmonic Generation (THG) imaging of hemozoin using ultra-fast (femto-second), infra-red pulsed laser excitation. THG is a material–dependent non-linear optical effect that involves conversion of fundamental laser frequency to a tripled frequency due to third-order dielectric susceptibility of the material. The results showed that hemozoin yields up to three orders of magnitude stronger THG signal than any other component found in blood. This is because hemozoin contains a condensed phase of iron (III) porphyrin rings which have an extensive polarizable β-electron system as opposed to iron (II) porphyrin rings found in haemoglobin.

Yulia et al. [22] used UV-visible spectroscopy to study intra-erythrocytic stages of Plasmodium falciparum. Using the first derivatives of the absorption spectra, they enhanced the differences in the absorption spectral features of infected red blood cells.

They observed an absorption peak centered at 650 nm whose size increased as the parasites progressed from ring to schizont stage. This peak was due to hemozoin. They also observed that the characteristic oxy-haemoglobin doublet at 540 nm and 575 nm in the haemoglobin spectrum was more pronounced in trophozoite stages but reduced in the schizont stage. The reduction in this doublet is the result of degradation of haemoglobin into the polymeric form of heme (hemozoin).

Webster et al. [23] Discriminated intra-erythrocytic stages of Plasmodium falciparum by employing synchrotron Fourier Transform Infra-Red (FT-IR) micro-spectroscopy in conjunction with principal component analysis. In FT-IR difference spectra between uninfected and infected erythrocytes, they observed bands assigned to hemozoin moiety 1712 cm^{-1}, 1664 cm^{-1} and 1209 cm^{-1}. By

employing principal component analysis to investigate spectra of parasites at different stages, they found that these bands were important contributors in separating between spectra of infected and non-infected erythrocytes.

Such a requirement is untenable for application in poor countries where malaria is endemic because they are very expensive. In addition, malaria diagnostics based on exclusive hemozoin detection may miss ring stage of Plasmodium since hemozoin is more pronounced in the mature trophozoites and schizont stages of Plasmodium.

In this thesis, Linani Dickson Omuchenia [24] develops method for rapid detection of Plasmodia (malaria parasites) in unstained thin blood smears has been developed. The method is based on microscopically imaging red blood cells using different wavelengths of light in the UV, visible and NIR region for illumination (an emerging field known as multispectral imaging microscopy).

The limitation of this work is pegged on inability of humans to classify the parasites in unstained smear. Since ANN is a supervised pattern recognition technique, its inputs were based on correctly classified cells from dark-field microscopy and PCA. Also need long time experience.

Dave M. Newman designed A prototype, computer controlled, non-invasive magneto-optic (NIMO) device based on MOT principles was constructed. It incorporates a dc electromagnet delivering a 0.5 T magnetic field across the nailbed. The optical beam is provided by a thermoelectrically cooled 120 mW 658 nm laser module expanded to an 8 mm diameter to ensure tissue-safe laser operation and incident onto the finger nail.

The advantages of this method view that Magnetic response of hemozoin in live parasitized red blood cells as a function of hemozoin concentration and (inset) applied magnetic field showing greater than 75% response obtained at fields less than 0.5 T, So this information about magnet power will help us in our research and must be taken.[30]

2.3 **body anatomy and its interaction with electromagnetic wavelength**

Snell [25], describe content of hand and its anatomy and divide it to:

- Skin
- Muscles
- Bones and joints
- Nerve and blood vessels
- Lymphatic system

Also he comprised skin into three main layers: epidermis, dermis and subcutis as depicted in Figure (2.6).

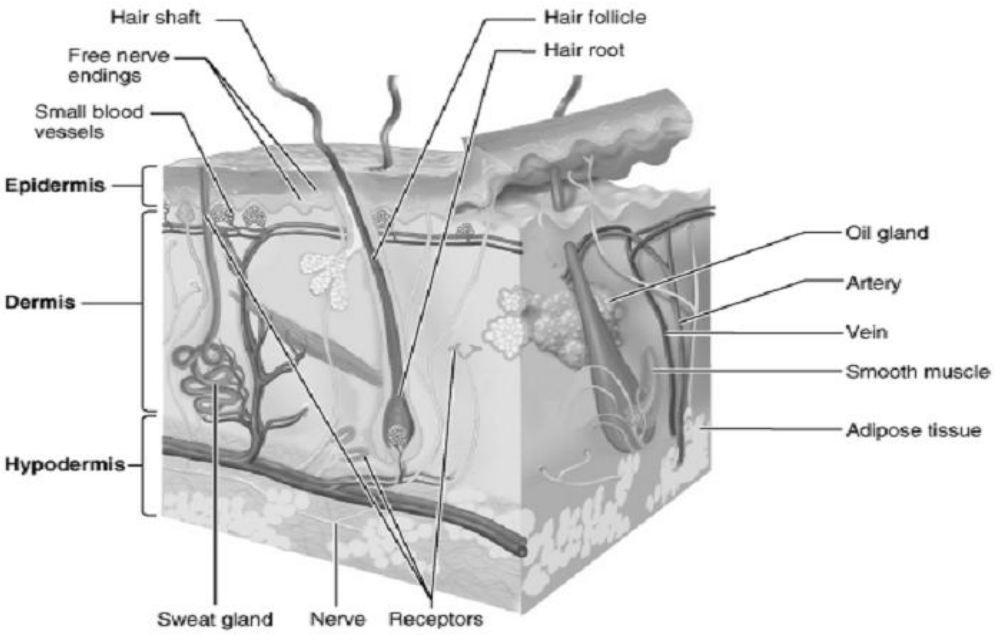

Figure (2.6): Human Skin Modeling and Rendering with electromagnetic wavelength

Pieter van der Zee [26] and Guillaume Poirier [29] determine the optical properties of brain tissue that govern the transport of light through tissue and develop a model for light transport in tissue that makes it possible to predict various parameters of clinical interest. These parameters are the effective optical path length for light transmitted through tissue, needed for the purpose of quantities spectroscopy, and the light distribution in tissue produced by an external light source in order to determine the deposited dose and for the study of imaging through tissue.

To this end, Pieter van der Zee measure the absorption and scattering properties of brain tissue as a function of wavelength with Monte Carlo model. This model gives a full 3-D simulation of light transport, and takes into account secular reflection and refraction at the tissue boundaries.

Nakajima, Pulse Oximeter [27], is an instrument that actually makes use of the variation in light absorption that occurs with each heart beat. In a pulse oximeter the transmission of light through tissue (in most cases the finger) is measured to detect the small pulsatile variation with each heart beat. This signal arises from the change in volume of the arterial blood vessels in the tissue, so calculation from the spectral characteristics of the pulsatile component reflect only the arterial haemoglobin saturation independent of light absorption by static tissue chromophores.

These final three papers help us to know and understand anatomy and physiology and determine light characteristics (absorption and scattering) of human body.

Chapter three

Theoretical background

In this chapter, a brief resume is given of the absorption and scattering characteristics of the near infrared region in biological tissues with magneto optical technology. Also some terms and concepts which will be used in later chapters are introduced. Throughout this work the wavelength will be expressed in units of nm is given together with a general perspective of UV-visible-NIR spectroscopy. The concept of Magneto Optical Technology (MOT), which are the cornerstones of this thesis, are also are discussed.

3.1 Light interaction with human body

The interaction of light with tissue in the near infrared region can mainly be characterized by two phenomena's: absorption, and scattering.

Absorption: Is a process where the energy of a light photon is taken up by a molecule without the re-emission of another photon (assuming that one ignores the thermal photons resulting from the heating caused by the energy absorption).

Scattering: Are processes where the initial direction of a photon changes due to an interaction with a scattering object. Two types of scattering can be distinguished: inelastic and elastic. In this section some of the general features of light scattering will be discussed. For elastic scattering some theory necessary for its description will be given together with a number of methods to calculate the single scattering properties of various types of particles.

3.1.1 Absorption theory

In a non-scattering homogeneous medium with an absorber present, the loss in intensity due to absorption as light travels through the medium is given by the Beer Lambert law:

$$\frac{I_{out}}{I_{in}} = e^{-\mu_a * d} \quad (3.1)$$

Where I_{in} is the intensity of the incident light, I_{out} is the intensity at distance d (mm) from the input, and μa is the absorption coefficient for that medium in mm^{-1}. The inverse of μa, 1/μa can be taken to be the absorption length. [38]

The effectiveness of a compound as an absorber is given by its extinction coefficient, also named specific absorbance, Ɛ (mm^{-1}.$Molar^{-1}$). This is equal to its absorption coefficient per unit of concentration in Molar. The absorption coefficient for a single compound at a given concentration c is therefore given by:

$$\mu_a = C\mathcal{E} \quad (3.2)$$

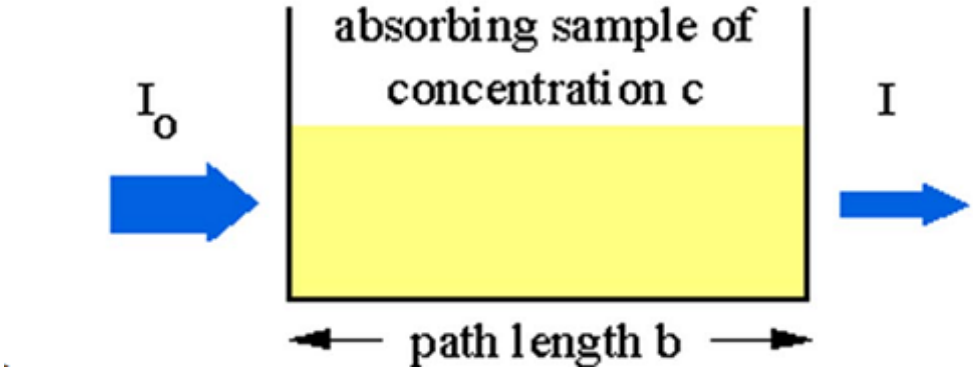

Figure (3.1): light travels through the medium as absorption interaction

Transmission will be described by equation (3.3) and absorption (attenuation) is described by equation (3.4):

$$T = \frac{I}{Io} \quad (3.3)$$

Absorbance (attenuation, or optical density):

$$A = -\log T \quad (3.4)$$

3.1.1.1 Water optical characteristics

Water is the most abundant chemical substance in the human body, accounting for 60 to 80 % of total body mass. The water content varies with tissue type and is age and gender-dependent. For example, the new-born brain comprises 90% water by mass, whereas the water content in adult skeletal muscle is around 74%. Because of its high concentration in most biological tissue, water is considered to be one of the most important chromospheres in tissue spectroscopy measurements. The region of low absorption acts as a 'window' of transparency, allowing NIR spectroscopic measurements through several centimeters of tissue to be made. [4]

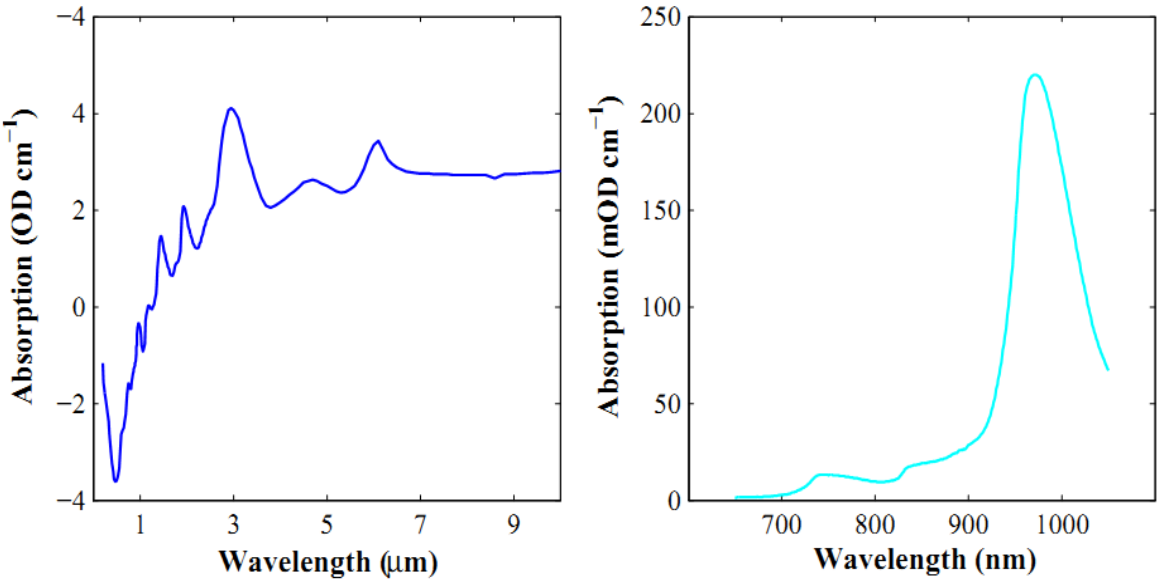

Figure (3.2): The absorption spectrum of pure water. Left: plotted on a log10 scale from 200 - 1000 nm, Right: the NIR region from 650 - 1050 nm

3.1.1.2 Haemoglobin optical characteristics

Within the water window of transparency the most dominant absorption of NIR light is by haemoglobin in its various forms. Haemoglobin is carried in red blood cells, or erythrocytes, and constitutes approximately 40–45% of whole blood. It is responsible for delivering oxygen from the lungs to the body tissues and returning

waste gases, such as carbon dioxide, to the lungs to be exhaled. Haemoglobin consists of the protein globin bound to four haem groups.

The absorption of oxy- and deoxyhaemoglobin, shown in Figure (3.3) has significantly deference, particularly in the red region of the visible and the NIR. This deference in absorption explains the visible color deference between venous and arterial blood. Arterial blood, which in adults is usually about 98% oxygen saturated, is bright red, whereas venous blood, which is approximately 75% saturated, appears dark red to purple in color. Although the NIR absorbance is reduced in amplitude relative to those in the visible, the spectra are still sufficiently deferent to distinguish between the two forms of haemoglobin. [38, 39, 40]

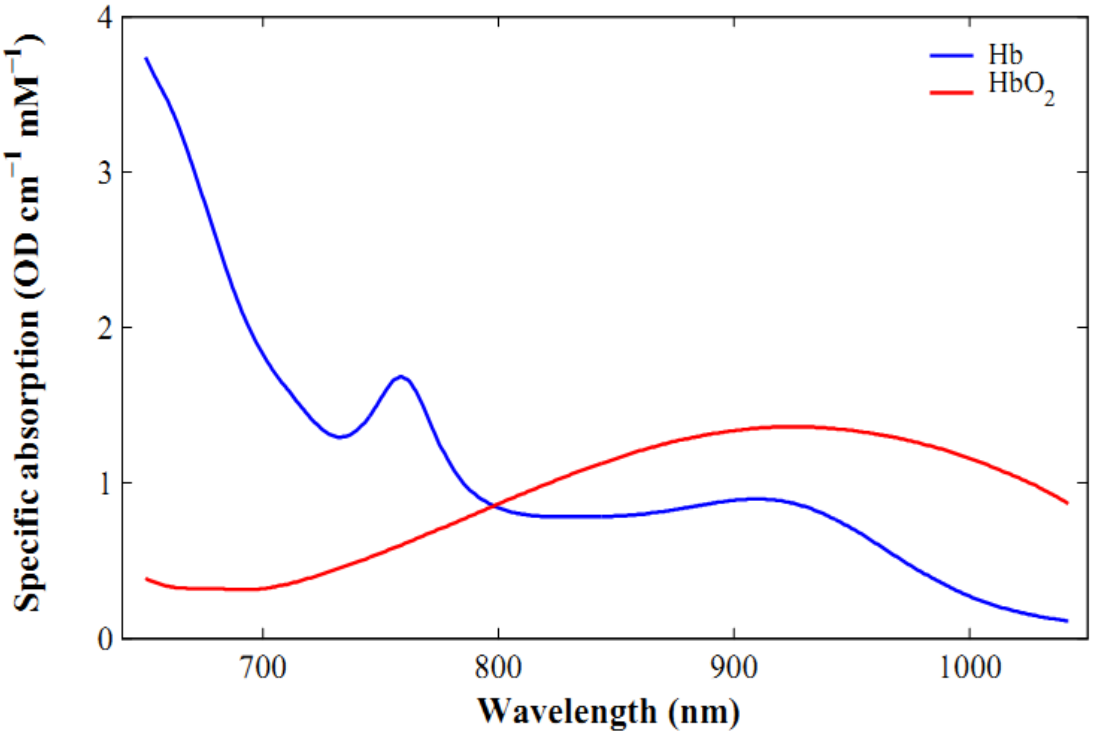

Figure (3.3): Specific absorption spectra of Hb and HbO2 in the NIR from 650 - 1050 nm.

3.1.1.3 Lipids optical characteristics

Most of the lipid in the body exists in the form of triglycerides (neutral fats) and is found in subcutaneous tissues and around internal organs. Phospholipids, another

group of lipids, are the main component of cell membranes and are thus found in every organ in the body. [38, 39]

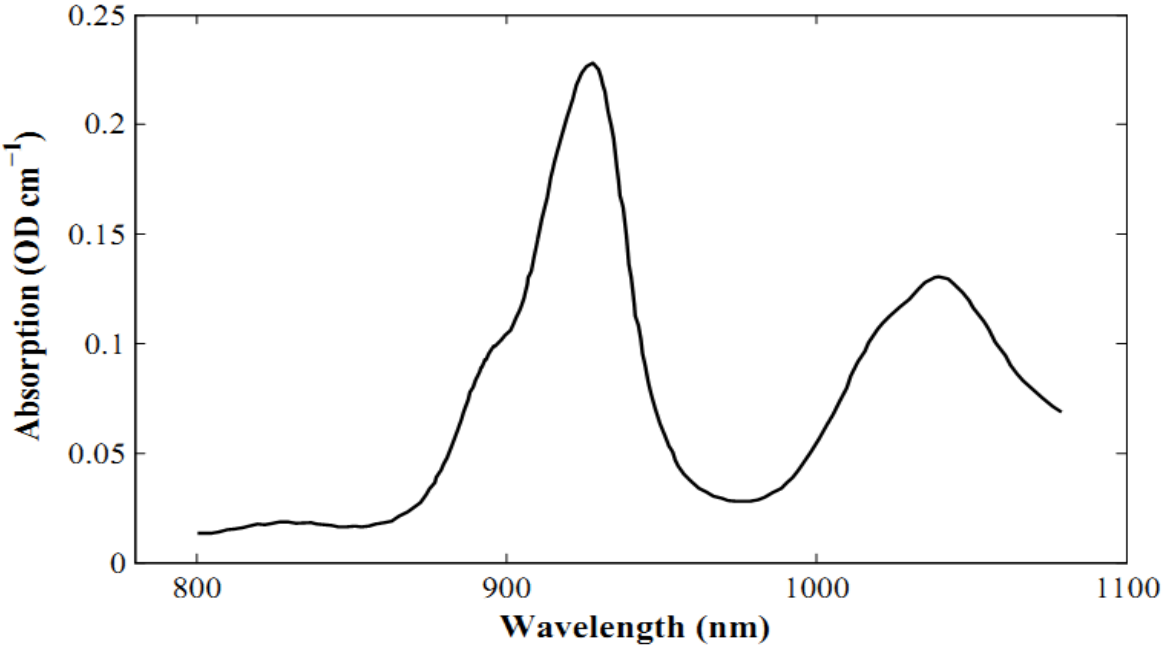

Figure (3.4): The absorption spectrum of pork fat (lipid) in the NIR from 800 - 1080 nm

We only discussed water, hemoglobin and lipids because there are a completely effect on light entry high concentrated which eliminate another affection of components. Such as Water content in adult skeletal muscle is around 74% and hemoglobin constitutes approximately 40–45% of whole blood. [4, 38, 39]

3.1.2 Light Scattering

Elastic scattering of light occurs when charged particles in a medium are set into oscillatory motion by the electric field of the incident wave, and re-emit (as opposed to absorb) light of the same frequency as the primary wave. Scattering occurs at non-resonance frequencies; hence the scattered intensities are relatively weak, since the forced vibrational amplitudes of the particles are much smaller than those at natural resonances. In most solids and liquids, however, intermolecular interactions broaden the absorption frequencies such that both scattering and absorption of light occur at all wavelengths.

As a result of scattering, the velocity of light in all matter is less than it is in vacuum. In an optically dense or homogeneous medium, i.e. one in which the molecular separation is much smaller than the wavelength of the incident light, individual atoms or molecules in a medium will scatter the incident radiation in all directions. The phase deference of the scattered light relative to the primary wave will depend on the frequency of the primary wave. In any direction the total scattered field is then a superposition of all the scattered wavelets propagating in that direction. The scattered waves will interfere with the incident wave, modifying its phase and hence the velocity of the light through the medium. [4]

Snell's Law

Snell's law (also called Descartes' law) [36] gives the relationship between angles of incidence and refraction for light impinging on an interface between two media with deferent indices of refraction, shown in Figure (3.5) The law follows from the boundary condition that a light wave is continuous across a boundary, which requires that the phase of the wave be constant on any given plane, resulting in

$$\eta_i (\lambda) \sin \theta_i = \eta_t(\lambda) \sin \theta_t \qquad (3.5)$$

Where:

η_i : index of refraction of outer media at wavelength λ,

η_t : index of refraction of inner media at wavelength λ,

θ_i : angle from the normal of the incident wave, and

θ_t : angle from the normal of the refracted wave.

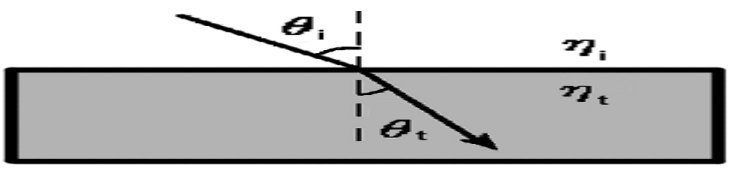

Figure (3.5): Snell's Law.

The refractive index of a medium is given by:

$$n = \frac{c}{v} \tag{3.6}$$

Where c: is the speed of light in vacuum and v: the speed of light in the medium. The refractive index depends on the number of molecules per unit volume and their polarisability, since the total scattered wave that interferes with the incident wave depends on the amplitudes of, and phase relations between, the individual scattered wavelets. [36, 39]

Rayleigh Phase Function

The Rayleigh phase function is used when the particle radius is somewhat smaller then the wave-length of light. Klassen [38] suggests that Rayleigh scattering should be used when r $\lambda < 0.05$.

Rayleigh scattering can model the scattering behavior of cigarette smoke and dust. For skin,

Rayleigh scattering is used to model the scattering of light by small-scale collagen structures in the dermis (Section 3.2.).

Rayleigh phase function is:

$$P_{Rayleigh}\cos(\alpha) = \frac{3}{4}(1 + (\cos\alpha)^2) \tag{3.7}$$

Mie Phase Function

The Mie phase function is used when the particles radius is comparable to the wavelength of light. Mie scattering can model the scattering behavior of water droplets or fog. For skin, Mie scattering is used to model the scattering of longer wavelengths in the dermis (Section 3.2.). Nishita et al. [39] propose two approximations for Mie scattering. The first one, hazy Mie, is used when the particle density is sparse. The second one, murky Mie, is used when the particle density is high.

The hazy Mie and murky Mie approximations are:

$$P_{hazyMie}\cos(\alpha) = 1 + 9\left(\frac{(1+\cos\alpha)^8}{2}\right) \tag{3.8}$$

And

$$P_{murkyMie}\cos(\alpha) = 1 + 50\left(\frac{(1+\cos\alpha)^{32}}{2}\right) \quad (3.9)$$

3.2 Absorption and scattering in human tissue

Absorption during exercise is more, so all below values will be at resting or normal case. [39, 40]

3.2.1 Skin:

The main layers are:

1. Dermis
2. Epidermis

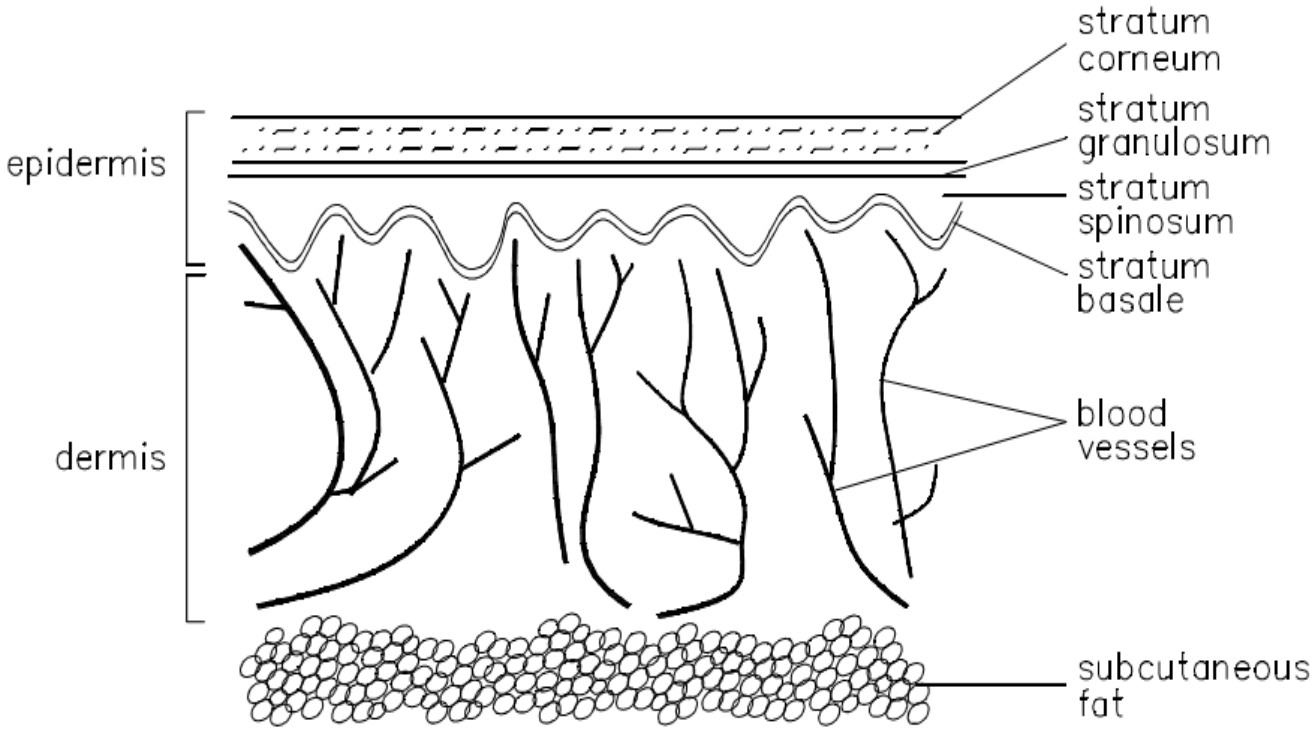

Figure (3.7): anatomical structure of the skin layers

Table (3.1): light properties of the skin layers

Layer	Thickness	properties
Stratum corneum	8-15µm	$\mu_s = 250\ mm^{-1}$ $\mu_a = 10\ mm^{-1}$ g = 0.9
Others	100µm	$\mu_s = 50\ mm^{-1}$ $\mu_a = 4\ mm^{-1}$ g = 0.75
Dermis	2-4 mm	$\mu_s = 20\text{-}50\ mm^{-1}$ $\mu_a = 0.2\text{-}0.5\ mm^{-1}$ g = 0.7-0.9

3.2.2 Blood

The most scattering is due to RBCS. There are also small contributions from the leucocytes, the platelets and from the large albumin molecules. For the scattering by red blood cells the shape of these cells has to be taken into account. The red blood cell is normally a regular doughnut shape (a biconcave disk), with a mean diameter of approximately 8 µm and a thickness varying from 1-2 µm.

Parameters:

- Typical values for the optical parameters are determined from Mie scattering for sphere at 685 ηm:

  $\mu_s = 20\text{-}50\ mm^{-1}$

  $\mu_a = 0.2\text{-}0.5\ mm^{-1}$

  g = 0.7-0.9
- Determined from Steinke and Shephard, at 633 ηm:

$\mu_s = 160\ mm^{-1}$

g = 0.985

3.2.3 Bones:

Particularly in the near infrared region, bone is found to be more transparent than most tissues. This is because although bone causes considerable scattering, there is in general little absorption except from haemoglobin in the blood inside the bone. With the exception of some of the larger bones, the blood content is low.

Parameters:

A recent set of measurements for pig skull over the range of 650 to 950 ηm gives values:

- g = 0.925 at 650 ηm to 0.945 at 950 ηm.
- μa = 0.04 mm^{-1} at 650 ηm to 0.06 mm^{-1} at 950 ηm.
- μs = 35 at 650 ηm and 24 mm^{-1} at 950 ηm.

3.2.4 Muscle tissue:

Muscle cells contain myoglobin as cytochrome. Total blood volume ≈ 0.5 ml\100gbut during exercise its 2ml\100g.

- For muscle the wavelength of absorption is 515 ηm, $\mu_a = 1.12 \pm 0.18 mm^{-1}$, $\mu_s = 53 \pm 4.4\ mm^{-1}$
- At 630 ηm, $\mu_a = 0.15\ mm^{-1}$, $\mu_s = 0.7\ mm^{-1}$ and g =0.954±0.016.
- Above 630ηm, $\mu_a = 0.166\ mm^{-1}$, μ_s (1 g) = 0.438 mm^{-1}.
- At 1064 ηm, $\mu_a = 0.118\ mm^{-1}$, μ_s (1 g) = 0.281 mm^{-1}.

Chapter four

Design and implementation

This chapter consists of methodology, mathematical model, block diagram, circuit diagram, source, detectors and whole component selection of the research.

4.1 Methodology

The methodology focuses on design and implementation of portable Prototype to detect malaria parasite depending on basis of mathematical modeling (absorption and scattering co-efficient of human tissue)using magneto optical technique (MOT) and embedded systems, by detecting IR wavelength using a data acquisition system to acquire the signal from human finger.

4.1.1 The steps of this research consist of:

- Design a black box with four sides from Teflon material with entering circular pin for finger entering and using a ring shape permanent magnet and LASER infrared source which are applied to the hemozoin molecules around finger (these inside box).
- Measure small changes in light wavelength and produces a voltage output using four linear array photodiode detectors (1^{st} for absorption at 90˚ from source, 2^{nd} for reflection behind IR source, 3^{d} detectors at left and right side of the absorption detector)**.**
- Convert an output current signal from each detector to output voltage using current to voltage converter.
- De-noise and amplify an output voltage using series of quad non-invasive Amplifier and filters (summing and average amplifier) with dc filter (band pass filter).

- Using Microcontroller to calculate hemozoin density from scattering, reflecting and absorption wavelength and make a decision of diagnose.
- Display the best measurement system and diagnosis decision on LCD.

4.2 Block diagram

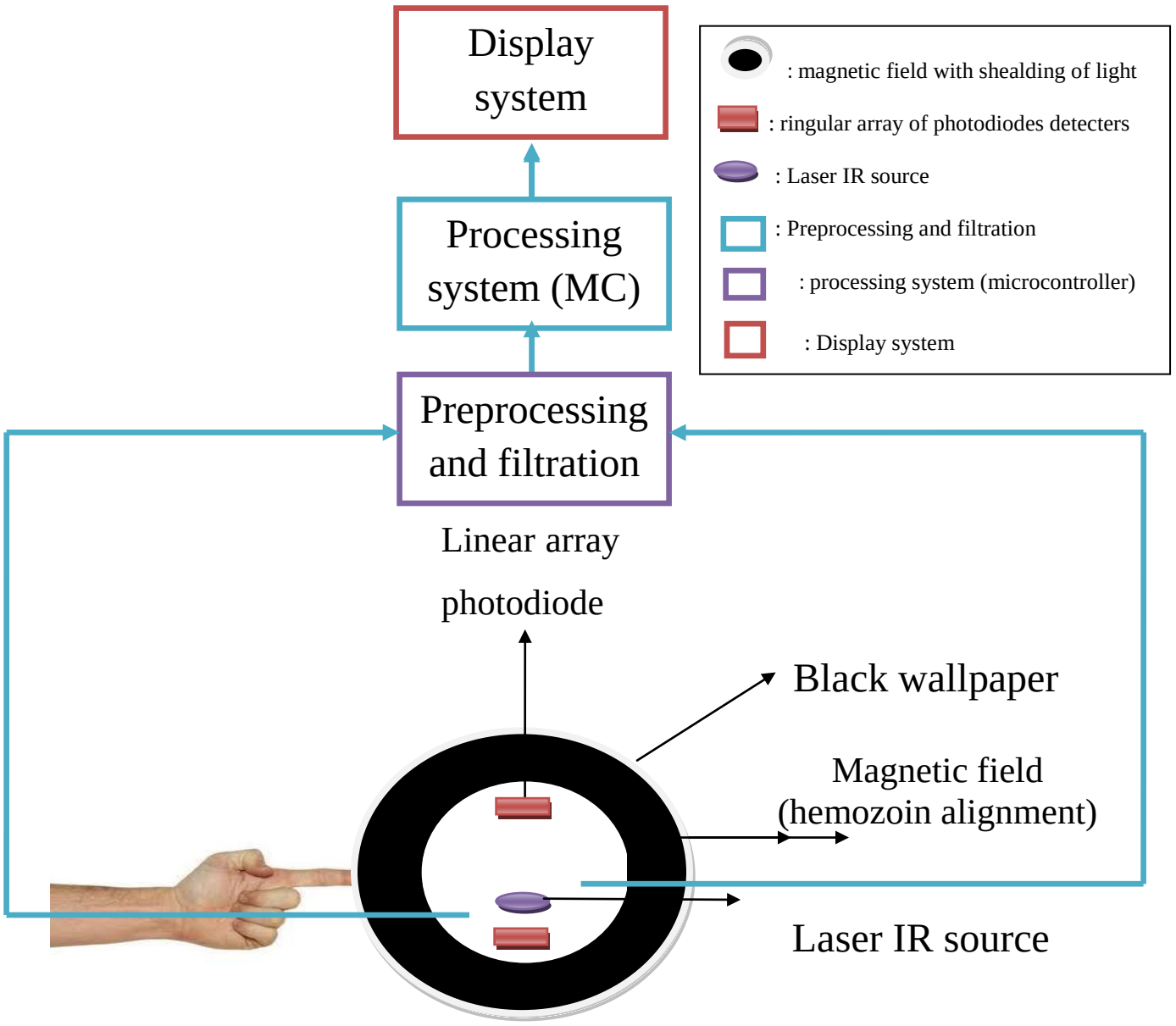

Figure (4.1 a): block diagram of non-invasive malaria detection system

4.3 Design model

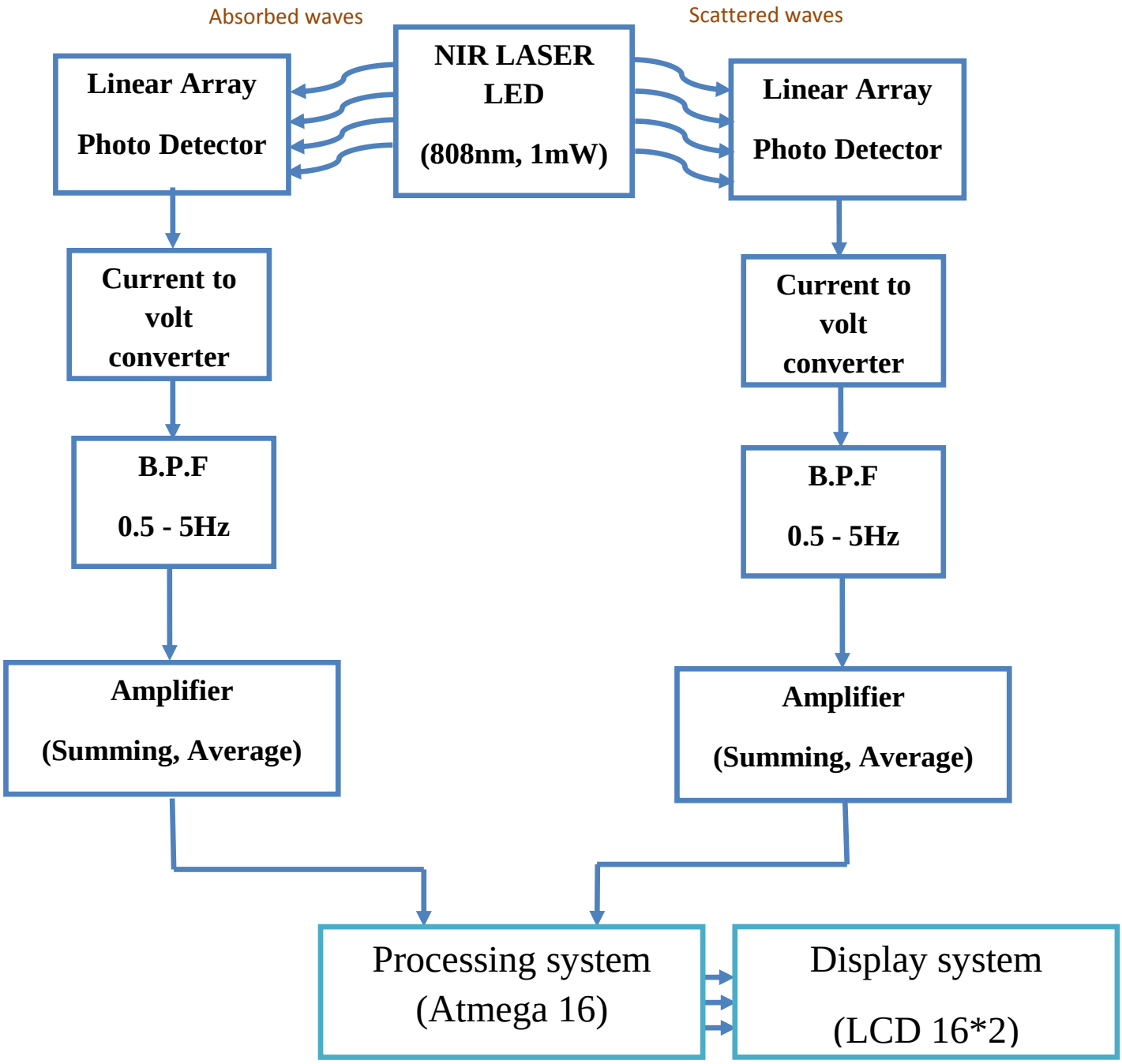

Figure (4.1b): block diagram of non-invasive malaria detection system with details steps

The block diagrams (4.1a) and (4.1b) above display of the malaria detection system components individuals as we will discuss from section (4.5) beginning with chamber design end with LCD at the end of this chapter.

4.4 Mathematical model (calculation for one case)

1. Wavelength source is 808 nm.
2. Complete width of the thumb is 20 mm.
3. Distance between source and thumb is 32mm, in addition thumb to detectors is 32mm.
4. Calculations done depend on Mie and Millar const.

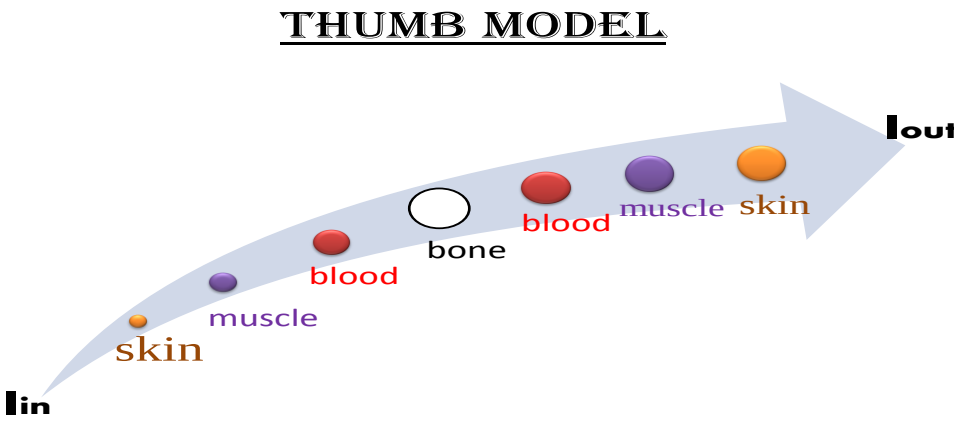

Figure (4.2): thumb model and layers

Table (4.1): scattering and absorption coefficient of thumb finger

Layer	Thickness (d)	Absorption coefficient (μ_a)	Scattering coefficient (μs)
Stratum corneum	8-15µm	$\mu_a = 10\ mm^{-1}$	$\mu_s = 250\ mm^{-1}$
Others skin	100µm	$\mu_a = 4\ mm^{-1}$	$\mu_s = 50\ mm^{-1}$
Dermis	2-4 mm	$\mu_a = 0.2\text{-}0.5\ mm^{-1}$	$\mu_s = 20\text{-}50\ mm^{-1}$
Muscle	1-2mm	$\mu_a = 0.166\ mm^{-1}$	$\mu_s = 0.438\ mm^{-1}$
Blood	8 µm	$\mu_a = 0.2\text{-}0.5\ mm^{-1}$	$\mu_s = 20\text{-}50\ mm^{-1}$
Bone	10 mm	$\mu_a = 0.06\ mm^{-1}$	$\mu_s = 24\ mm^{-1}$

At normal:

1. **Skin:**

$$Io = I_{in}\, e\, -\sum \mu_a * d \qquad (4.1)$$

- ✓ Stratum μa=10 mm^{-1} of 10 μm:

$$(10*10*10^{-9})=10^{-6}$$

- ✓ Dermis μa= 0.35 mm^{-1} of 3mm :

$$(0.3*0.35*10^{-9})=1.05*10^{-3}$$

- ✓ Others μa= 0.4 mm^{-1} of 100 μm :

$$(4*100*10^{-9})=0.4*10^{-6}$$

$$\therefore \text{Total skin} = \sum \mu_a * d = 0.0010514$$

$$\therefore I_o = Iin*e^{-0.0010514}$$

2. **Muscle:**

- ✓ μa=0.118 mm^{-1} of 1 μm:

$$(0.118*10^{-3}*10^{-6})=10^{-6}$$

3. **Blood:**

- ✓ μa=0.35 mm^{-1} of 1.5 μm:

$$(0.35*10^{-3}*1.5*10^{-6})= 0.525*10^{-9}$$

4. **Bones:**

- ✓ μa=0.06 mm^{-1} of 2 mm:

$$(0.06*10^{-3}*1.5*10^{-3})= 0.09$$

$$\therefore Io = Iin*e^{-0.9}$$

Or

$$\therefore I_o = Iin*e^{-2(0.525*10-9)+(0.09)+2(10-6)+2(0.0010514)}$$

$$\therefore I_o == Iin*e^{-0.0921048105}$$

And again for skin, muscle and blood so we multiply it with 2.

Scattering:

At normal:

1. **Skin:** $I_o = I_{in}\ e^{-\sum \mu_s * d}$

- ✓ Stratum μs=250 mm^{-1} of 10 μm:

$$(10*10^{-6}*250*10^{-3})$$

- ✓ Dermis μs= 35 mm^{-1} of 3mm :

$$(3*10^{-3}*0.35*10^{-3})$$

- ✓ Others μs= 50 mm^{-1} of 100 μm :

$$(100*10^{-6}*50*10^{-3})$$

$$\therefore \text{Total skin} = \sum \mu_s * d$$

2. Muscle:

- ✓ μs=0.438mm^{-1} of 1 μm:

$$(10^{-6}*0.438*10^{-3}$$

Blood:

- ✓ μa= 35 mm^{-1} of 1.5 μm:

$$(1.5*10^{-6}*35*10^{-3})$$

3. Bones:

- ✓ μs=24 mm^{-1} of 2 mm:

$$(24*10^{-3}*1.5*10^{-3})$$

$$\therefore I_o = I_{in} * e^{-4.46029*10^{-5}}$$

So total scattering equation will be:

$$\therefore I_o = I_{in} * e^{-8.46059*10^{-5}} \qquad (4.2)$$

4.5 Chamber design

This chamber has main function blocking any interaction of light from outside environment and focus the selecting source only to the finger, which has below specification depend on finger length and diameter and magnet design**.**

This box was made of Teflon material and paint with black color to generate special environment that need for experiment, it has four sides each one has length 70mm , wide 62.5mm and also 70mm for highest. Other two sides is electric board base.

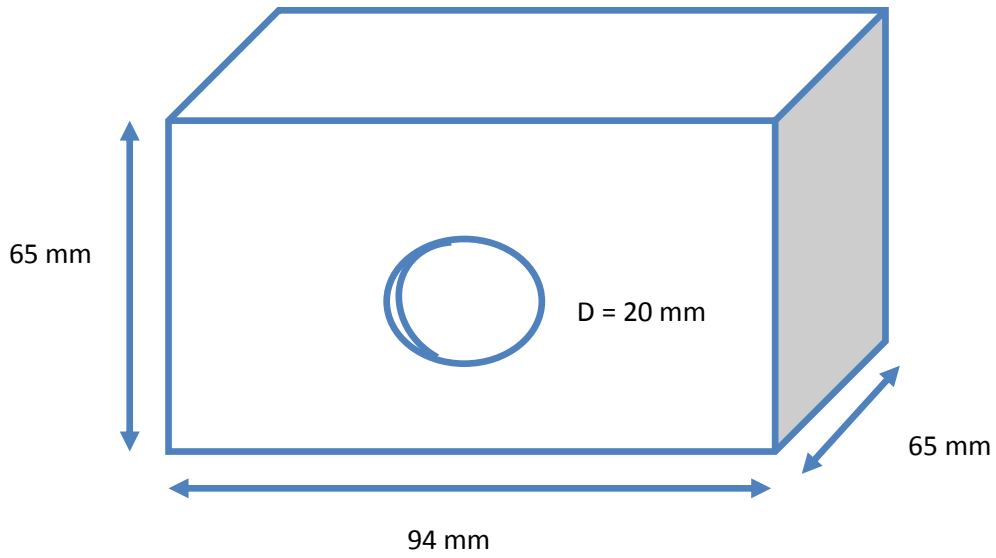

Figure (4.3): black chamber dimension

4.6 Source selection and its configuration circuit

Human tissue contain water, lipids and hemoglobin which has exists a region of relatively low absorption at electromagnetic wavelength between 200 and 900 nm , above 900 nm the absorption coefficient increases fairly rapidly to a peak at about 970 nm, and following a minor trough continues to increase at longer wavelengths into the mid- infrared.

To generate light signal that penetrate human body, IR wavelength with 808nm length was selected depend on low absorption factor in human tissue at this range (chapter three). Also to give exact degree of orientation for this wave with a few deviations to measure and differentiate between absorption, reflection and scattering a laser property will do this work, so final selection was a **laser diode**

submount 2.0w cw (c-mount): SPL CG81-2S that has low power 2Watt for painless effect.

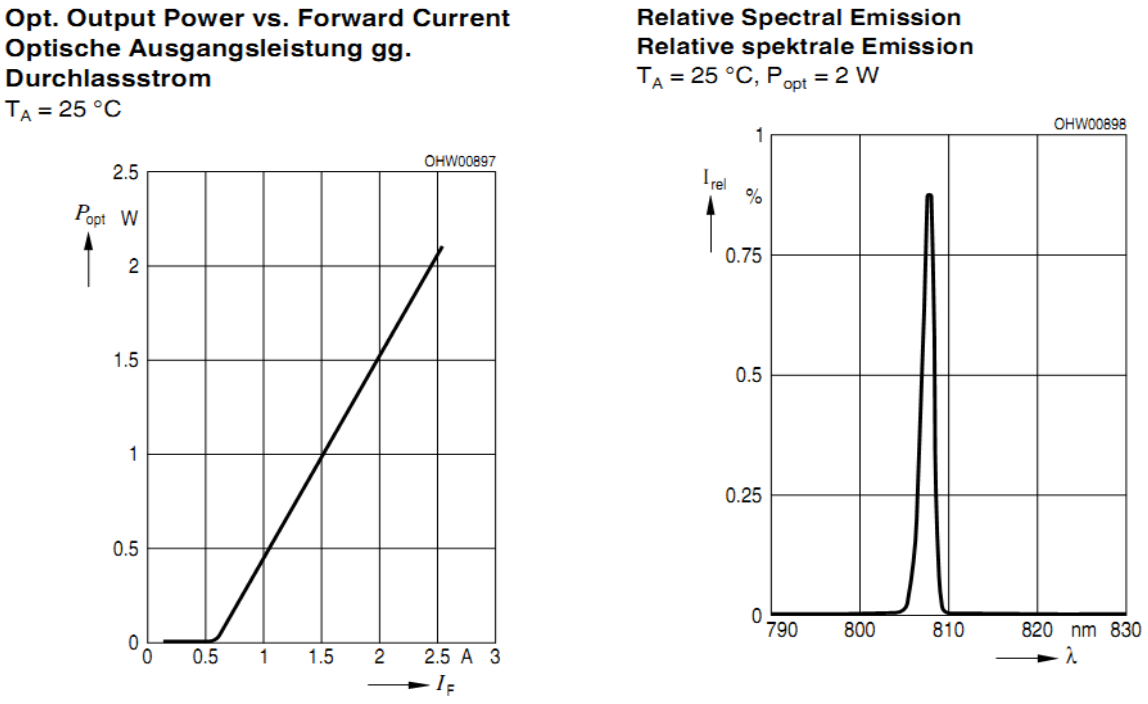

Figure (4.4): output power vs. foreword current and relative spectral emission for **SPL CG81-2S**

4.6.1 SPL CG81-2S Configuration

Parameter	Symbol	Values	Unit
Emission wavelength	λ_{peak}	808	Nm
Spectral width (FWHM)	$\Delta\lambda$	3	Nm
Peak output power	P_{out}	2	W
Threshold current	I_{thres}	0.6	A
Operating current	I_{oper}	2.35	A
Operating voltage	V_{oper}	1.9	V

4.6.2 Driving circuit for laser diode

From above table operating current must be between (2.35 to 2.6 A) and operating voltage (1.9 to 2.1V), that need two parallel dc battery 1.5 V with variable resistor (50M Ω) to generate exact resolution and sensitivity of wavelength. The transfer function of this circuit will represent as ohm's law:

$$V = I * R \tag{4.3}$$

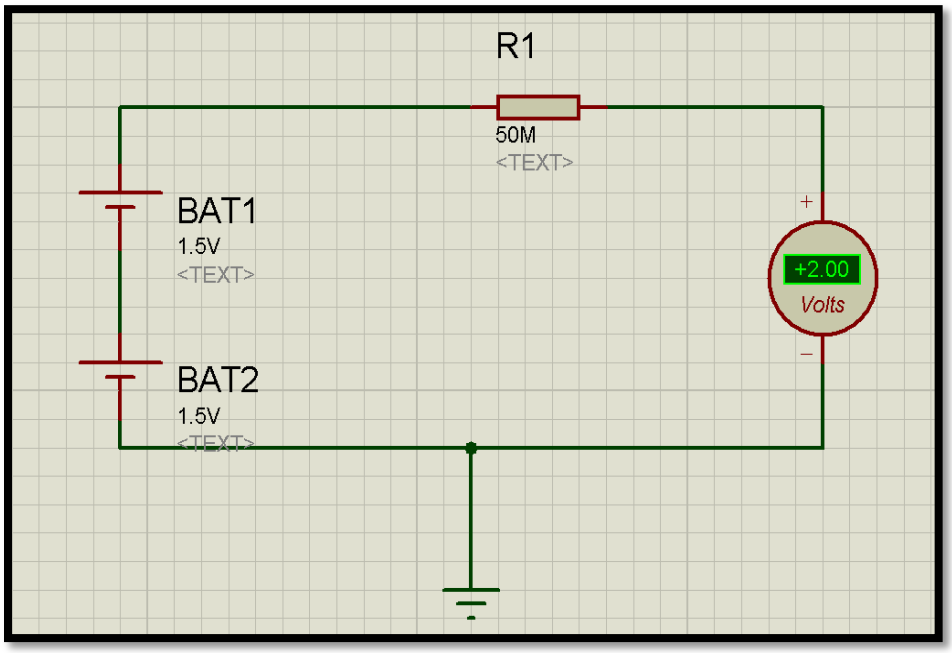

Figure (4.5): Driving circuit for laser diode

4.7 Detector selection and configuration

To detect this range of waves after biological interaction and give a change in its power spectrum, selection must taken into account the range of wavelength for source which must be included, so detectors will be SI Linear Array Photodiode(S4111-16R) which has sixteen photodiode in small distance for accuracy objective.

This detector has eighteen pins; two of them cathodes (KC) can be connected to negative voltage up to 15V for dual mode or ground. Other pins are anodes to give

an output current with mA scale. At this research only an output of six pins are taken into account five scattering and one for absorption wavelength.

Another one need for reflection behind source; also five element output will be taken to give reflection waves from finger.

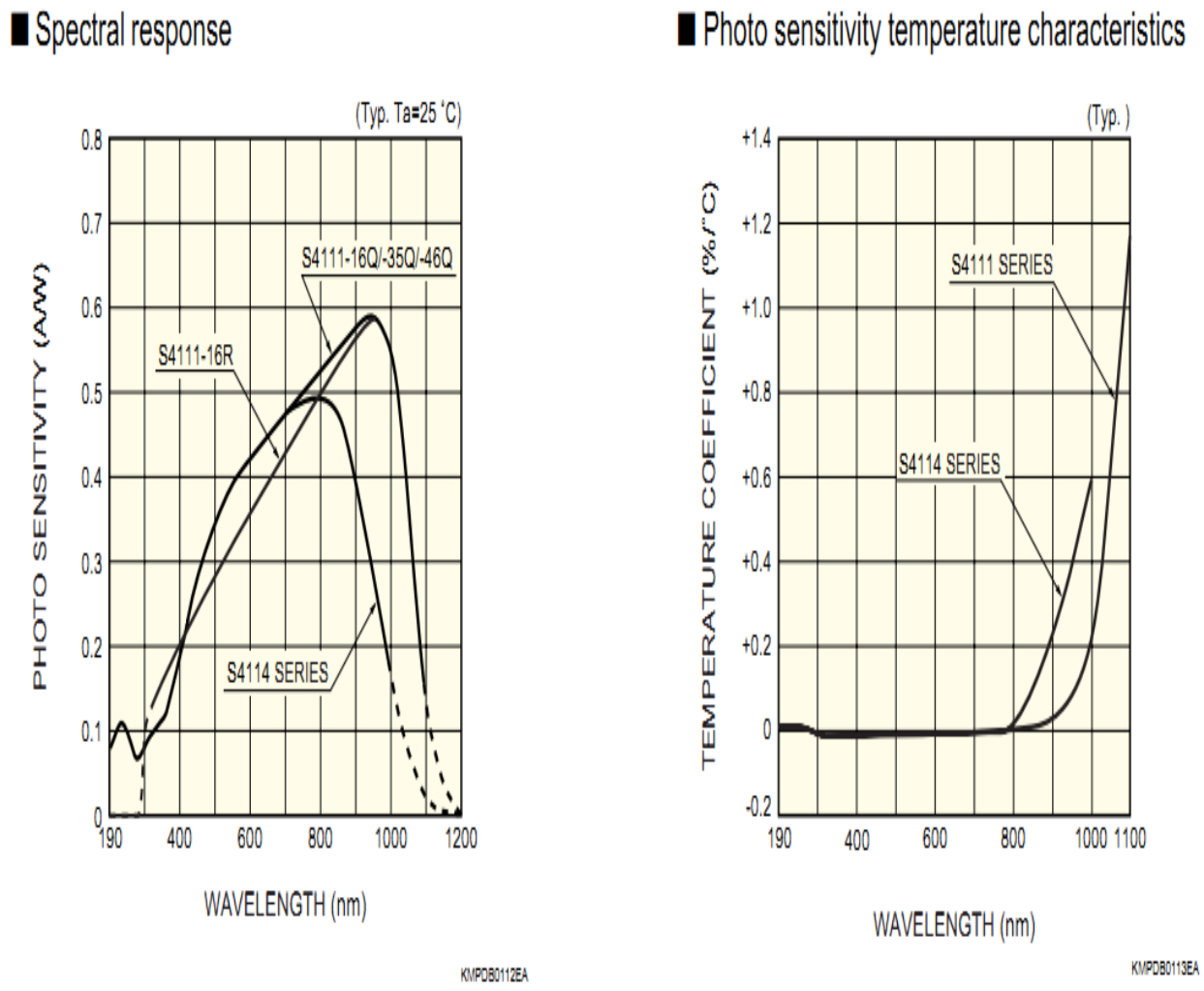

Figure (4.6): spectral response and photosensitivity temperature characteristics for S4111-16R detector

Table (4.3): pins connection of S4111-16R

Pin No.	16-element type
1	KC
2	2
3	4
4	6
5	8
6	10
7	12
8	14
9	16
10	KC
11	15
12	13
13	11
14	9
15	7
16	5
17	3
18	1

4.8 Output signals preprocessing

An output current from SI photodiodes array detector will be weak signal so their needs to convert firstly into voltage and after that entering amplification circuit which will be two stages in hypnoses with DC artifact rejection filter in each.

4.8.1 Current to voltage converter circuit

It's a circuit connection that gives an output voltage depending on entire current this circuit consists of: operation amplifier with feedback resistor only (no input resistor) and capacitor for dc filtration as rule below:

$$Vout = Iout * R \qquad (4.4)$$

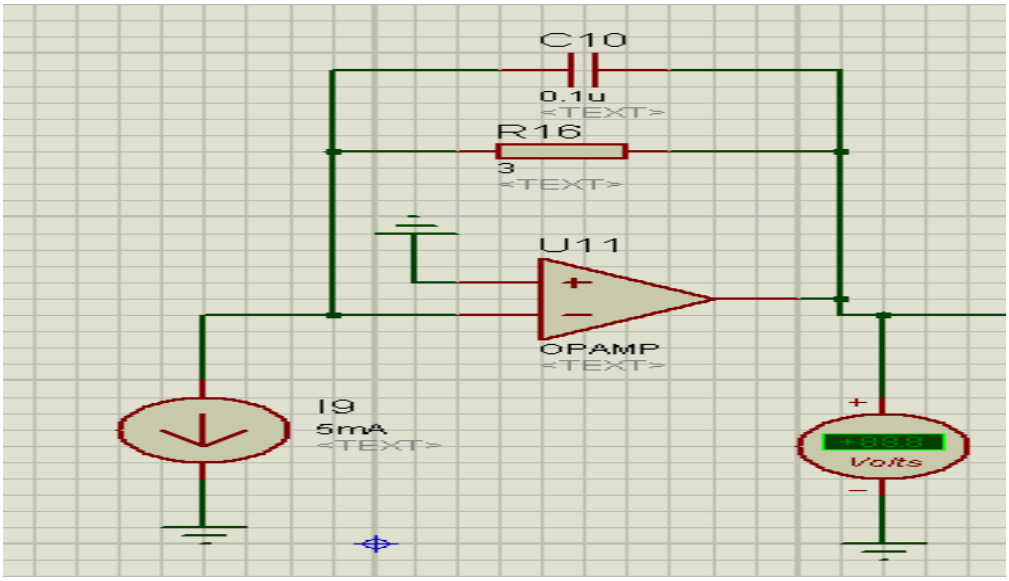

Figure (4.7): Current to voltage converter circuit

4.8.2 Absorption signal

Third and fourteen elements of the first SI detector will be an output for this function signal, which will enter the converter and take two amplification stages with gain(G=3*0.5*1.5=5),second stage is summing amplifier as seen in figure (4.8) below and then entre microcontroller pin number 35 (portA5).

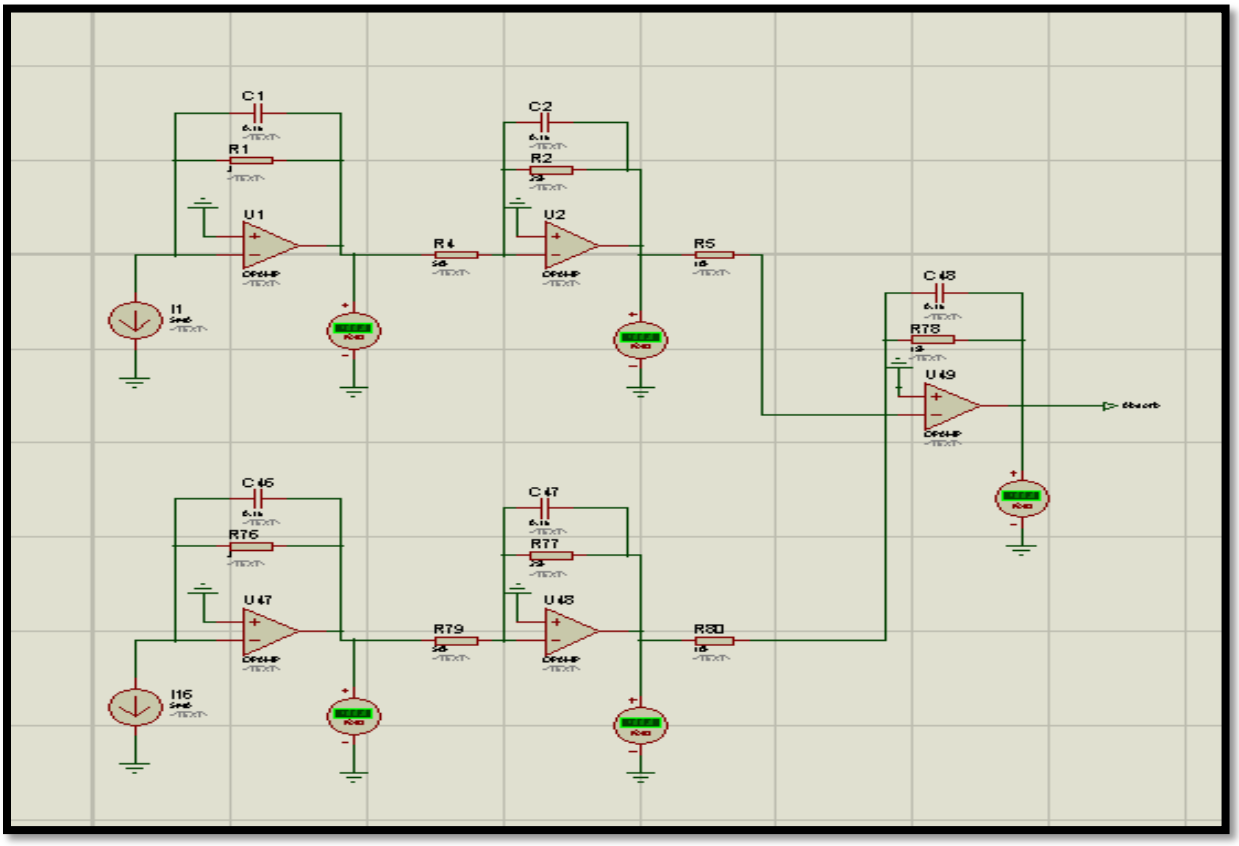

Figure (4.8): absorption detection and preprocessing circuit

4.8.3 Reflecting signal

Five elements from each side of the second SI detector will enter the converter and take first amplification stage with gain (G=2) which will entre second stage as summing amplifier (G=1.5) for all of it to represent reflecting signal from source as seen in figure (4.9) below and then entre microcontroller pin number 34 (portA6).

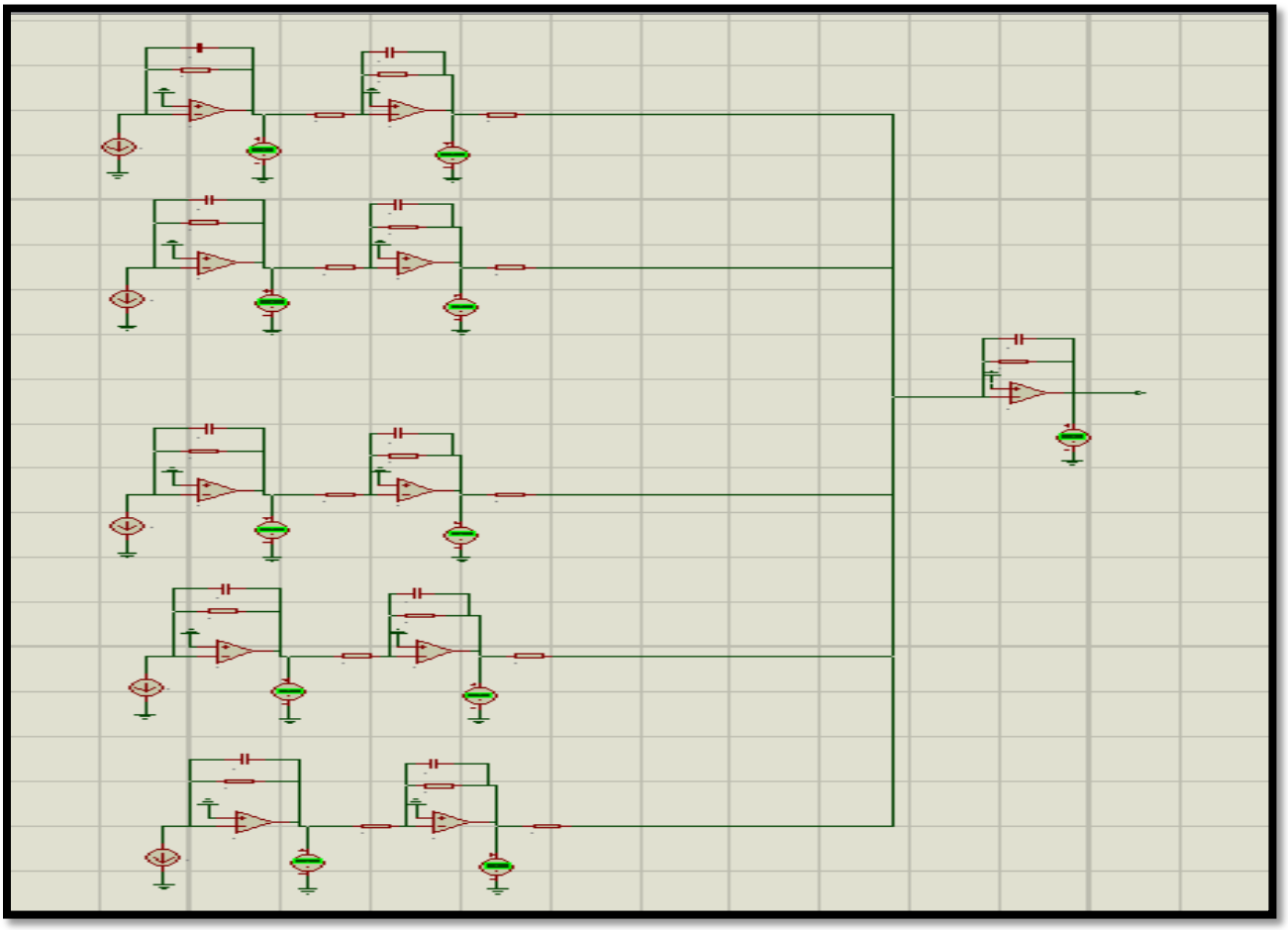

Figure (4.9): reflection signals detection and preprocessing circuit

4.8.4 Scattering signal

Ten elements five from each side of the first SI detector will be an output for this function signal, which will enter the converter and take first stage amplification with gain (G=3), then any parallel two elements will entre second stage summing amplifier (G=1.5+0.5=2) **to give five scattering signals** entre microcontroller pins from (potrA0 to portA4) each pin represent define scattering angle as seen in figure (4.10) below:

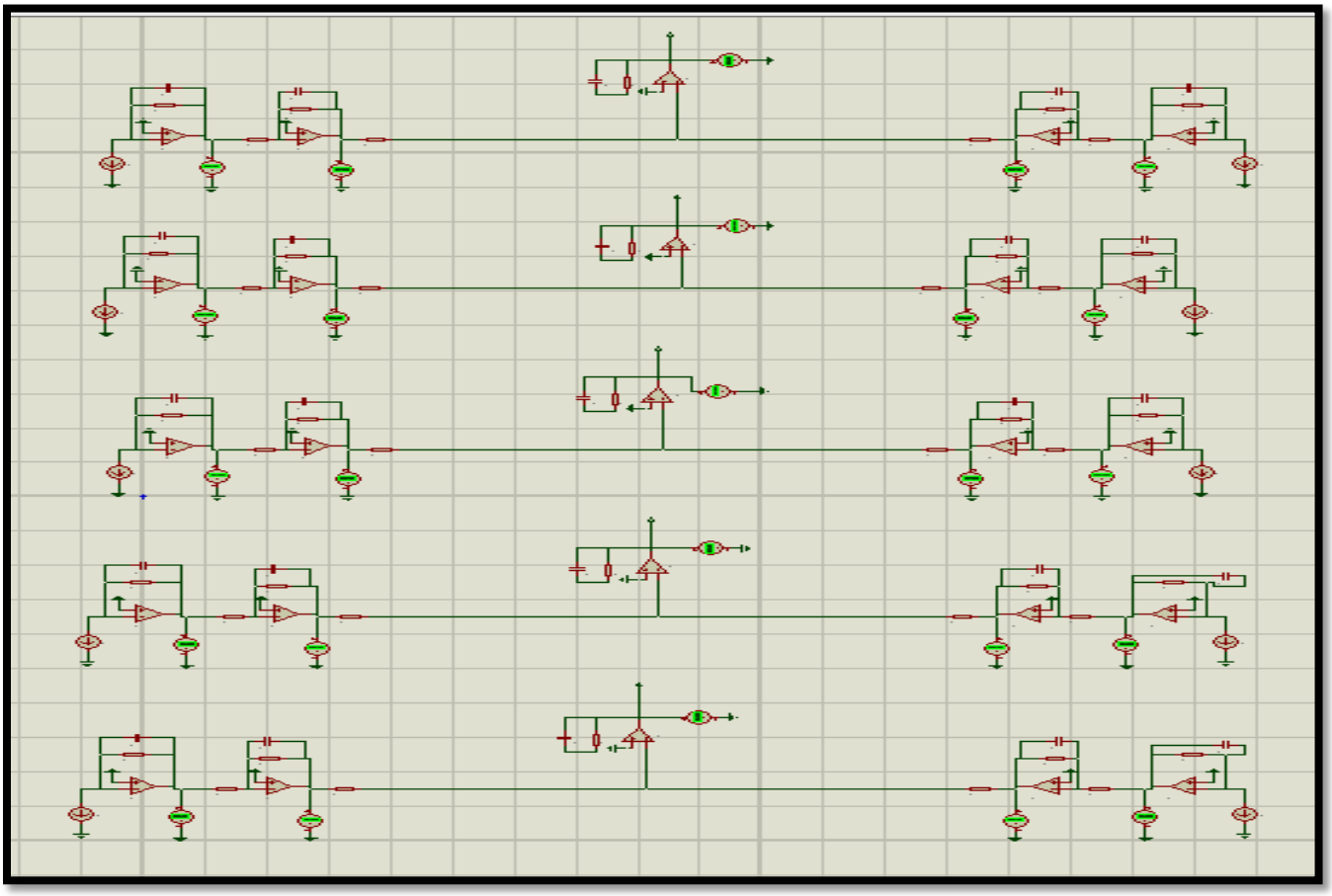

Figure (4.10): scattering signals detection and preprocessing circuit

4.9 Processing system (MC)

At this research a microcontroller ATmega 16 will be used to process the system and determine malaria non-invasively. The ATmega16 supports different design requirements and reduce cost; it has components that are useful for typical microcontroller applications, such as:

- Analog-to-digital converter,
- Pulse – width - modulator.

4.9.1 Specifications of ATmega16

	ATmega16
Number of instructions	131
Flash program memory	16K
Internal SRAM	1K bytes
EEPROM	512 bytes
External memory	none
General-purpose 8-bit registers	32
IO ports	4
Serial interfaces	SPI, USART, Two-wire
Timers	two 8-bit, one 16-bit
PWM channels	4
ADC	Analogue comparator, 8-channel 10-bit ADC
Interrupt vectors	21

Figure (4.11): ATmega16 pins and specifications

At this project we used port A as input for ADC (0x00) by entering an output of sensors into portA_0, A_1 ….A_6 and port D for output to display system LCD (0xff) by using:

Table (4.4): ADC pin configuration

Pins of port A	**Detector**
Pin 0	Scatter
Pin 1	Scatter
Pin 2	Scatter
Pin 4	Scatter
Pin 5	Absorb
Pin 6	Reflect

Inside the microcontroller, it must be a program to calculate light intensity values corresponding to the output voltage values from ADC and show result at LCD. From this step, the dissection of malaria detection will determine.

4.10 Design algorithm derivation

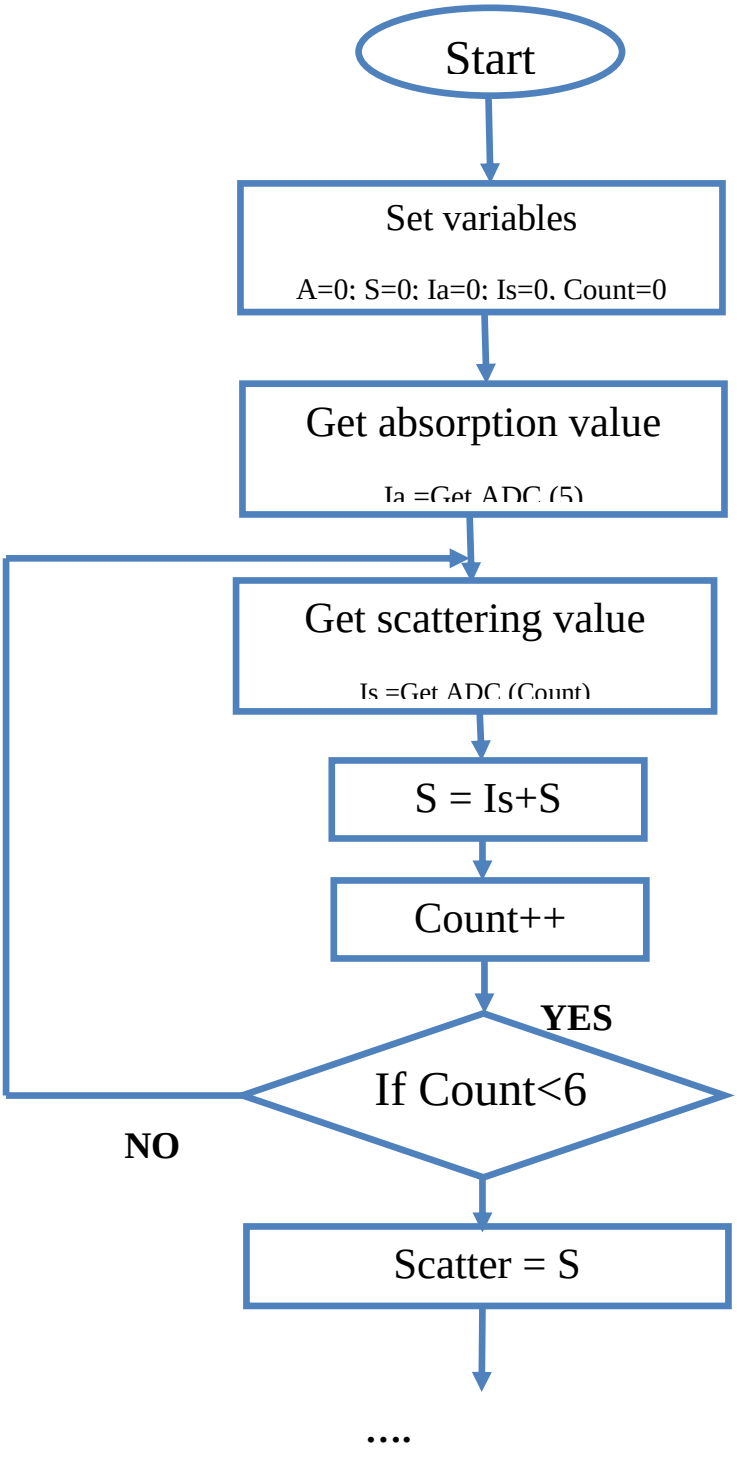

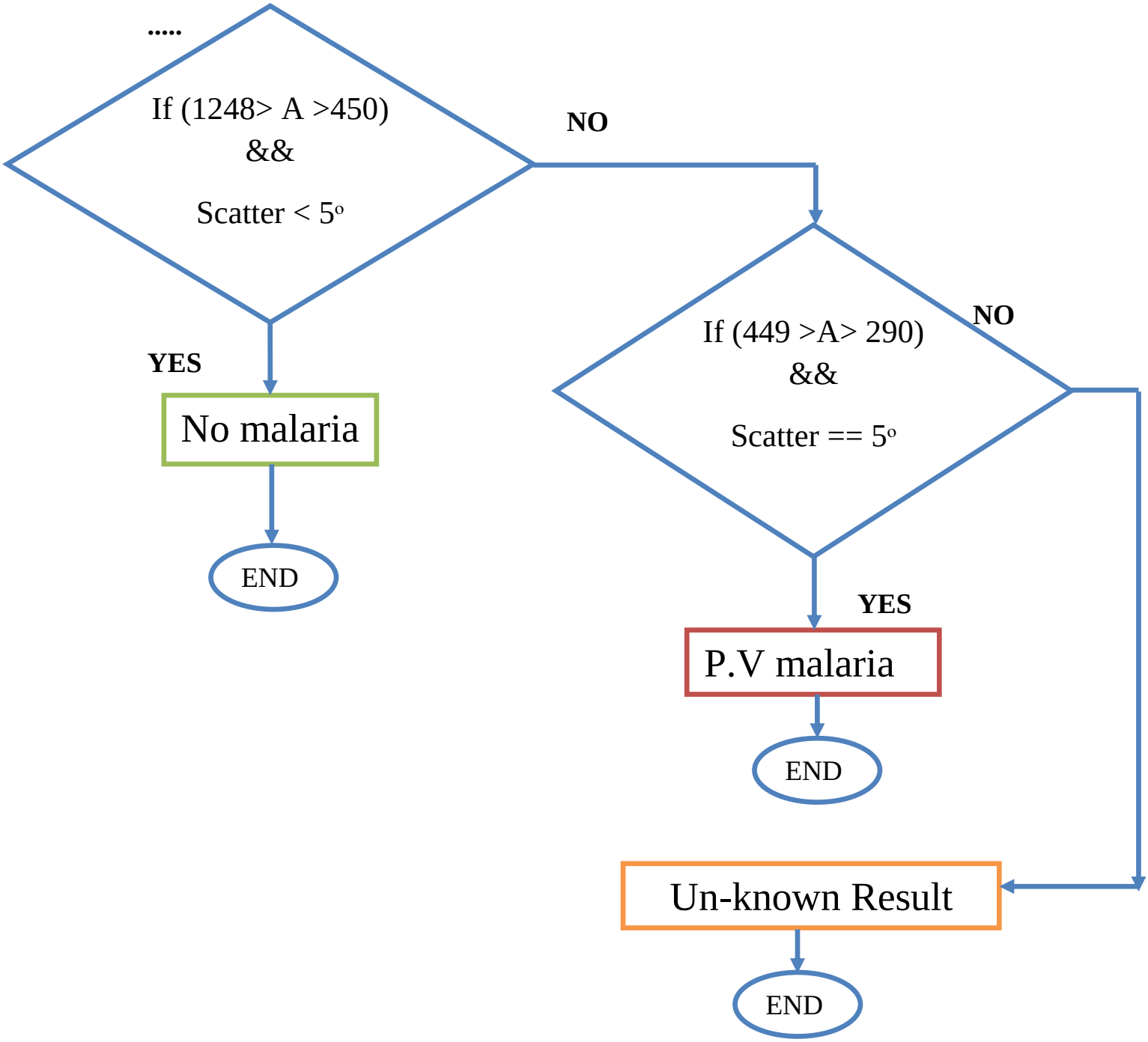

Figure (4.12): flow chart of Non Invasive malaria detection system.

The flow chart (4.12) above shows the steps of the software program of the proposed system which explain that how to decide founding of malaria parasite in the body by calculating of absorption (A for absorb) and scattering (S for counting scattering angles from 0 to 5 degrees) with a conditions of both values.

4.11 Display system

The system that selected for displaying is liquid crystal display sixteen columns in two rows, to view result in its screen after processing. To synchronize LCD showing with process mandatory to interface its pins with microcontroller as table (4.5) below:

Table (4.5): LCD pin interfacing with microcontroller.

Pins of port D	**LCD pins**
Pin 0	RS
Pin 1	WR
Pin 2	E
Pin 4	D_4
Pin 5	D_5
Pin 6	D_6
Pin 7	D_7

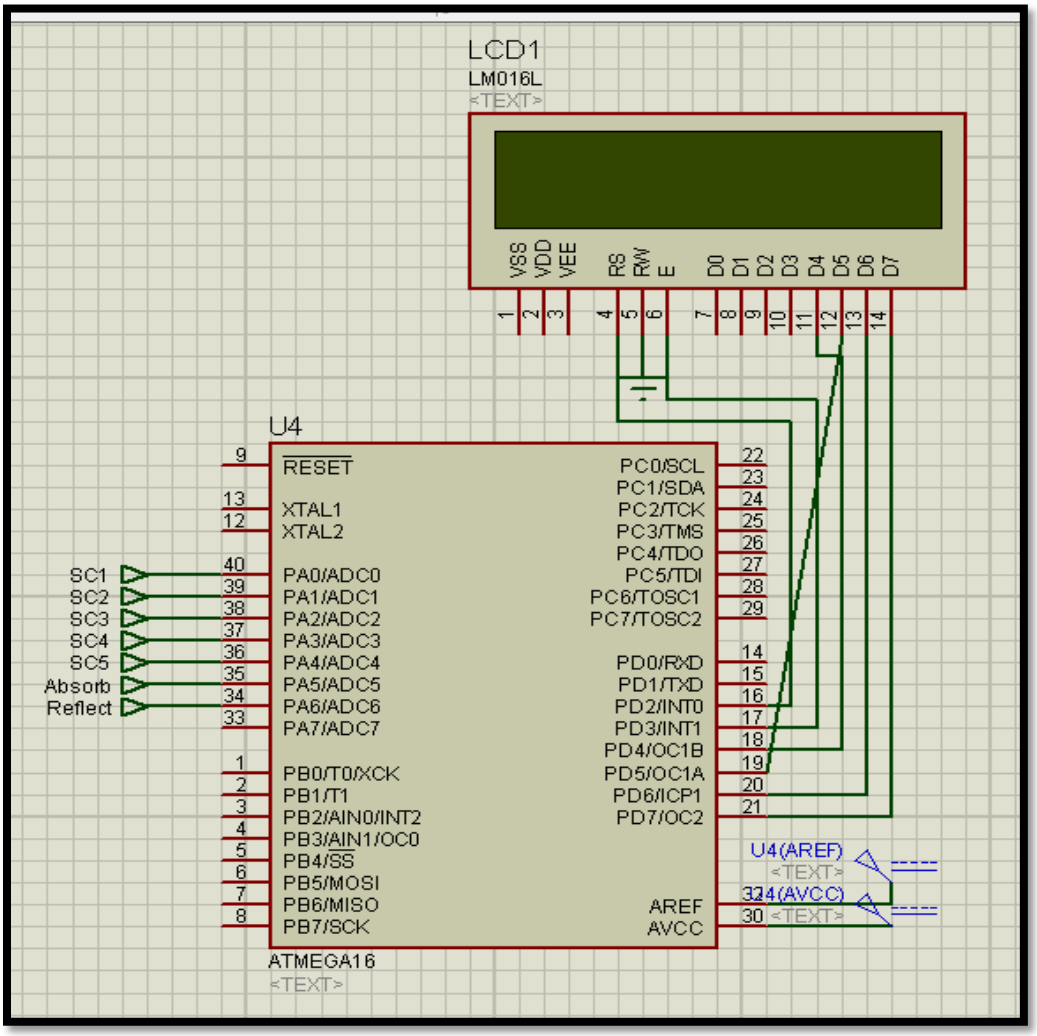

Figure (4.13): processing and display system with ATmega16 and LCD (LM016L)

4.12 Calculations

The intensities of detectors will change their value depending on the body interaction with light (absorption, scattering and reflection). A simple circuit will be used to convert these changes in intensity current to a voltage change. These voltage values will be sent to the microcontroller via ADC. We need do some math for ADC, Our reference voltage (V_{ref}) is 5V [35], and the ADC is 10 bit. So, any input voltage from (0 - 5V) will be mapped to a digital number between (0 - 1023). The resolution of ADC is:

$$ADC(resolution) = \frac{\text{refernce voltage}}{digital\ number} = \frac{5}{1024} \quad (4.5)$$

$$ADC(resolution\ ) = 0.004882 \text{ V/Count.}$$

Therefore, the digital output corresponding to any input voltage:

$$Vout = \frac{\text{Vin}}{0.004882} \quad (4.6)$$

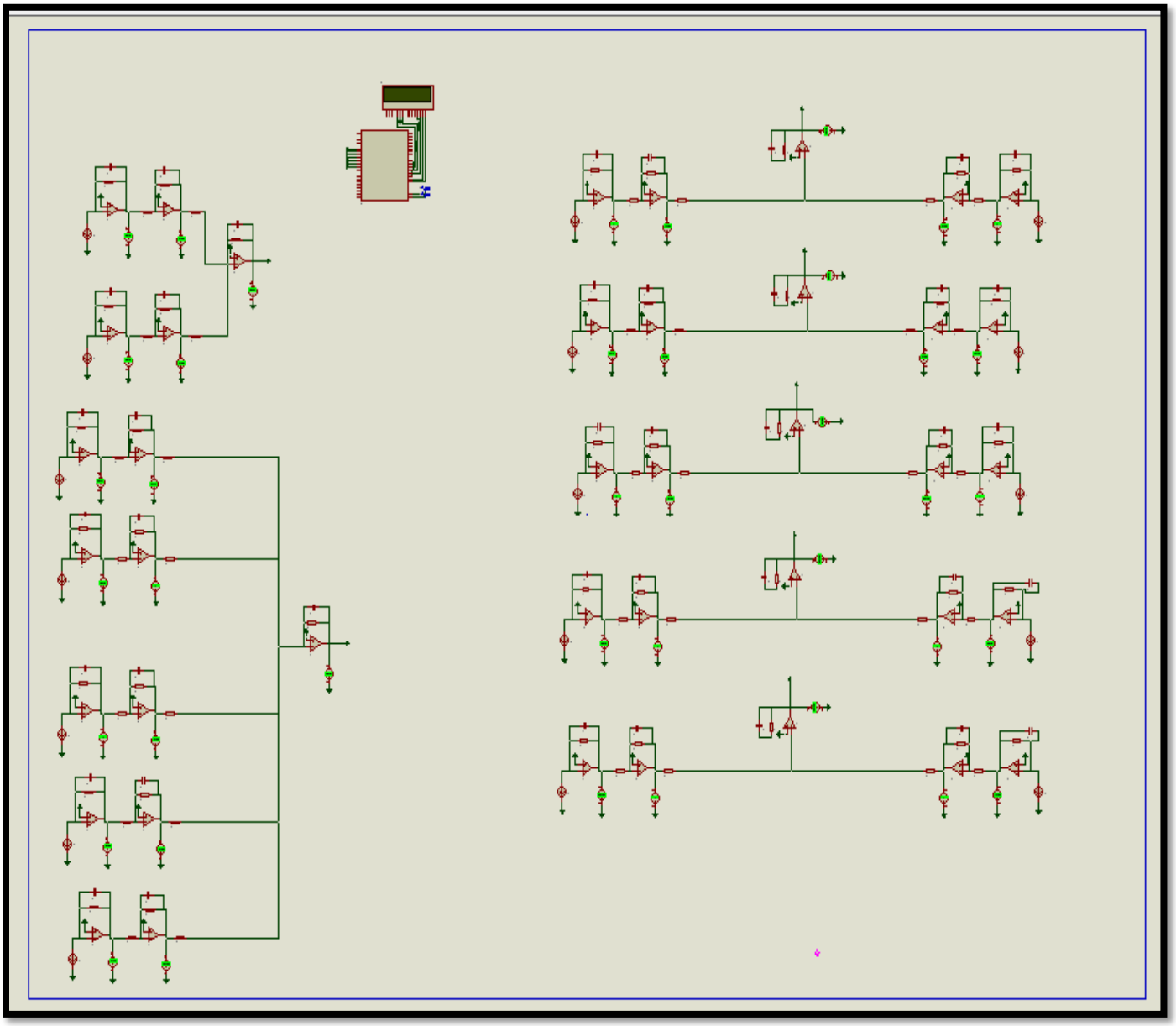

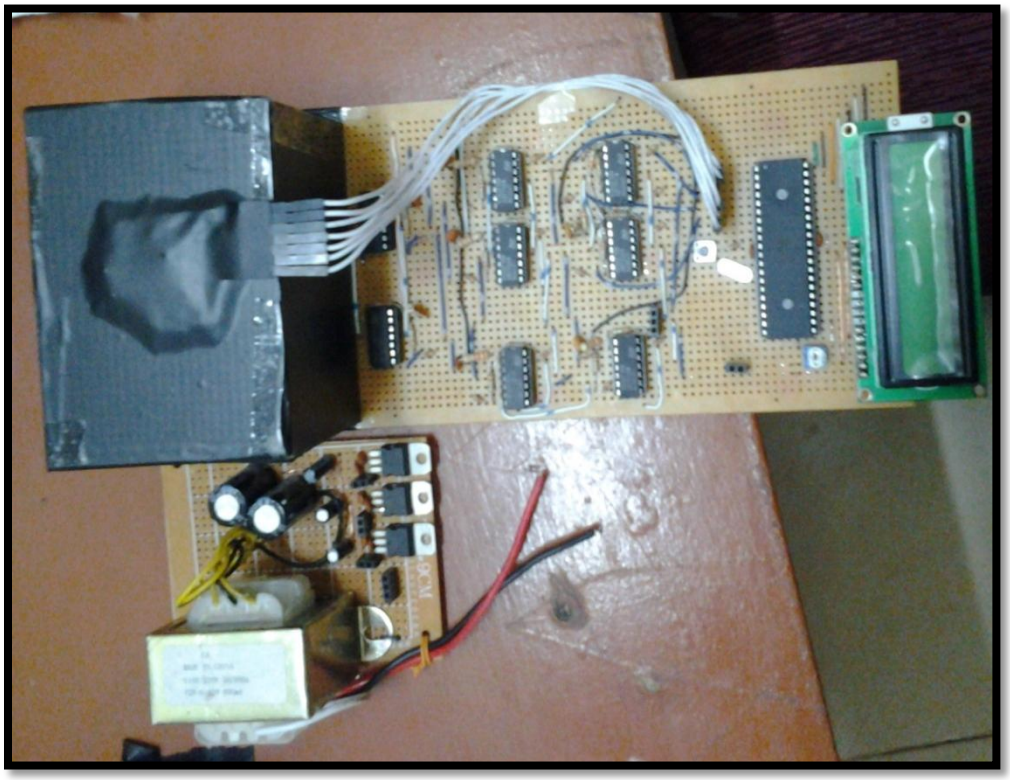

Figure (4.14): Circuit block diagram and design of non-invasive malaria detection system

4.13 Power supply of the system

The system above contains linear array detectors which need positive feedback (+ 9V) and negative feedback (- 9 V) in addition to LCD and microcontroller which need +5 V to work. So we need to design a power supply contain these three sources by using Transformer (12 V), bridge rectifier, regulators (+ 9V,- 9V and + 5V) and capacitors for filtration as figure (4.15) shown below:

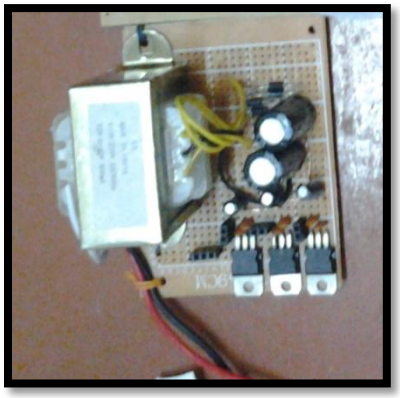

Figure (4.15): Power supply of the system

4.13 Statically Analysis of the system

After finding the results and compare it with laboratory we will find sensitivity and accuracy by calculating True positive value (TP) which is contains true positives, subjects with the disease and positive test results, True negative value (TN) that means subjects do not have the disease and the test agrees, False positive value (FP) identifies individuals without disease but for whom the test indicates 'disease'. These are false positives and false negative value (FN) has the false negatives.

Sensitivity is the probability that a test will indicate 'malaria' among those with the malaria:

$$\text{Sensitivity} = \text{TP}/(\text{TP} + \text{FP}) \times 100 \quad (4.7)$$

Accuracy

Accuracy is how close a measured value is to the actual (true) value.

$$\text{Accuracy} = \frac{\text{Number of correct samples}}{\text{Number of all samples}} * 100\% = \frac{47}{52} * 100 \quad (4.8)$$

Chapter five

Experiments Results

This chapter describe experiments set up and design, results of the system that conclude from fifty two experiments compare with laboratory results divide into normal (healthy) and illness (malaria disease) and displayed accuracy and sensitivity of the system.

5.1 Experiment considerations

To run this experiment volunteer must have finger diameter no more than twenty millimeters with applying of pressure for blood vessels around.

In addition to create a magnetic field (0.3 T) around finger to oriented hemezoin pieces inside RBCS in one direction (if it found) and save temperature range at normal conditions (37^{o}c), all these conditions to give accurate results showing in the display system .

5.2 System description

Fifty two persons at this experiment are females with aging range from (15 to 60) years. When volunteer insert his finger inside chamber a laser IR source (HLM1230,650nm,5mW) in replace to the SPL CG81-2S source (because it's not available to deliver to Sudan now) will produce in invisible light directly to the finger, some of these wavelength will penetrate finger after a few absorption, some is allying and scattered after entering and other reflect back to the above; all these signal will receipt with detectors called linear array photo detectors (S4111-16R) and then proceed as it show in chapter three to display result (normal or malaria case) at LCD.

5.3 run system

Firstly we will make a circuit configuration to find minimum and maximum values of absorption and scattering angles, after that we will find the best

method to identify malaria cases with high accuracy by comparing between measurements with and without magnet and pressure force and take the more efficient way for detection.

5.3.1 Circuit configuration

Table (5.1): Closed room with open source:

	1	**2**	**3**	**4**	**5**
Absorb	1248	1248	1248	1248	1248
Sc1	1248	1248	1248	1248	1248
Sc 2	1248	1248	1248	1248	1248
Sc 3	1248	1248	1248	1248	1248
Sc 4	1248	1248	1248	1248	1248
Sc 5	1248	1248	1248	1248	1248
Angle	5^{o}	5^{o}	5^{o}	5^{o}	5^{o}

Table (5.2): Closed room with closed source:

	1	**2**	**3**	**4**	**5**
Absorb	0	0	0	0	0
Sc1	817	818	795	802	819
Sc 2	0	0	0	0	0
Sc 3	0	0	0	0	0
Sc 4	0	0	0	0	0
Sc 5	0	0	0	0	0
Angle	0^{o}	0^{o}	0^{o}	0^{o}	0^{o}

As shown on table (5.1) Closed room with open source, we noticed that maximum values for absorption and five scattering angles are equal with (1.248 v), but with closed source all measured values are zero voltage except first scattering angle which has range from (795mV to 820mV), as shown in table (5.2) and this will be a new zero value of SC_1.

5.4 display result

5.4.1 without pressure

Table (5.3.a): display result without pressure

	1	**2**	**3**	**4**	**5**
Absorb	447	483	457	485	507
Sc1	588	643	507	499	626
Sc 2	546	426	445	428	566
Sc 3	564	472	445	472	463
Sc 4	546	502	509	585	466
Sc 5	460	408	506	584	453
Angle	5^o	5^o	5^o	5^o	5^o
Lab	No	No	No	No	No

Table (5.3.b): display result without pressure

	6	**7**	**8**	**9**	**10**
Absorb	456	330	270	9	0
Sc1	399	316	783	550	1041
Sc 2	396	426	1248	1248	1248
Sc 3	468	408	13	19	10
Sc 4	291	310	263	230	213
Sc 5	427	428	0	0	0
Angle	5^{o}	5^{o}	4^{o}	4^{o}	4^{o}
Lab	Yes	Yes	No	No	No

Table (5.3.c): display result without pressure

	11	**12**	**13**	**14**	**15**
Absorb	1248	1248	1248	1248	1248
Sc1	1026	1051	933	989	968
Sc 2	1248	1248	1248	1248	1248
Sc 3	234	0	0	125	126
Sc 4	241	168	250	261	291
Sc 5	0	0	0	0	0
Angle	4^{o}	4^{o}	4^{o}	4^{o}	4^{o}
Lab	No	No	No	No	Yes

Table (5.3.d): display result without pressure

	16	**17**	**18**	**19**	**20**
Absorb	338	1248	1248	1248	1248
Sc1	795	788	819	1110	1054
Sc 2	1248	1248	1152	1248	1248
Sc 3	2	0	13	212	12
Sc 4	157	0	153	195	0
Sc 5	1248	0	0	0	0
Angle	5^{o}	2^{o}	2^{o}	3^{o}	2^{o}
Lab	Yes	No	No	No	No

Without magnet and pressure many values appear as zero voltages and no variants between malarial and non malarial cases as shown in table (5.3).

5.4.2 With magnet and pressure force

Table (5.4): display result with magnet and pressure force

	1	2	3	4	5	6	7	8	9	10	11	12
Absorb	467	454	433	25	9	0	0	1248	1248	1248	1248	1248
Angle	2°	2°	2°	2°	2°	2°	2°	2°	5°	2°	5°	2°
Result	No	No	No	No	No	No	No	No	Yes	No	Yes	No
Laboratory	Yes	Yes	Yes	No	No	No	No	Yes	Yes	No	No	No

When we use a pressure equal to the volunteer pressure and constant value of magnet (0.3T) as we shown on table (5.3), the results will be more accurate as:

For normal (non malarial cases):

- Scattering angle value will vary from (1^{o} to 3^{o}).
- Absorption value will vary from (450 to 1248) mV.

For malarial cases:

- Scattering angle value will be always (5^{o}).
- Absorption value will vary from (290 to 449) mV.

5.5 Experiment results compare to laboratory results

After finding the best measuring method (measuring with pressure and magnet), a (52) volunteers readings were taken and compared with laboratory results as shown in table (5.5) to find accuracy and sensitivity of the system and its ability to replace invasive detection methods.

Table (5.5.a): experiment results compare to laboratory results

	1	2	3	4	5	6	7	8	9	10	11	12	13	14	15
Absorb	1248	1248	1248	1248	1248	1248	0	1248	1248	1248	1248	1248	467	454	433
Angle	2°	2°	3°	2°	5°	2°	2°	5°	5°	4°	2°	4°	5°	5°	5°
Result	No	No	No	No	Yes	No	No	Yes	Yes	No	No	No	Yes	Yes	Yes
Laboratory	No	No	No	No	No	No	No	Yes	Yes	No	No	No	Yes	Yes	Yes

Table (5.5.b): experiment results compare to laboratory results

	16	17	18	19	20	21	22	23	24	25	26	27	28	29	30
Absorb	25	9	0	428	428	389	432	463	458	430	428	458	380	433	406
Angle	4°	y5°	4°	5°	5°	5°	5°	5°	5°	5°	5°	5°	5°	5°	5°
Result	No	Yes	No	Yes	Yes	Yes	Yes	Yes	Yes	Yes	Yes	Yes	Yes	Yes	Yes
Laboratory	No	No	No	Yes	Yes	Yes	Yes	Yes	Yes	Yes	Yes	Yes	Yes	Yes	Yes

Table (5.5.c): experiment results compare to laboratory results

	31	32	33	34	35	36	37	38	39	40	41	42	43	44	45
Absorb	389	319	389	449	330	385	315	311	305	390	433	447	850	1248	1248
Angle	5°	5°	5°	5°	5°	5°	5°	5°	5°	5°	5°	5°	5°	2°	2°
Result	Yes	Yes	Yes	Yes	Yes	Yes	Yes	Yes	Yes	Yes	Yes	Yes	Yes	No	No
Laboratory	Yes	Yes	Yes	Yes	Yes	Yes	Yes	Yes	Yes	Yes	Yes	Yes	Yes	Yes	Yes

Table (5.5.d): experiment results compare to laboratory results

	46	47	48	49	50	51	52
Absorb	0	1248	126	449	270	9	0
Angle	2°	2°	3°	5°	4°	4°	4°
Result	No	No	No	Yes	No	No	No
Laboratory	No	No	No	No	No	No	No

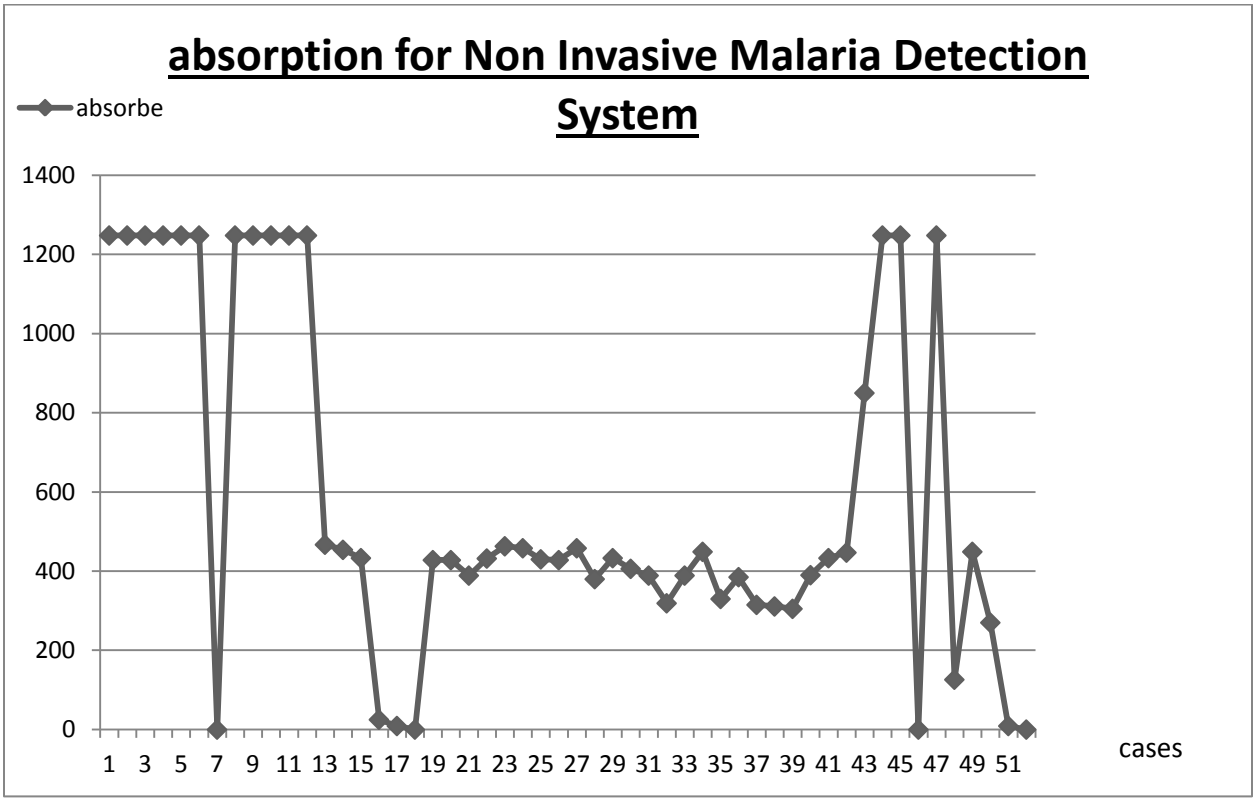

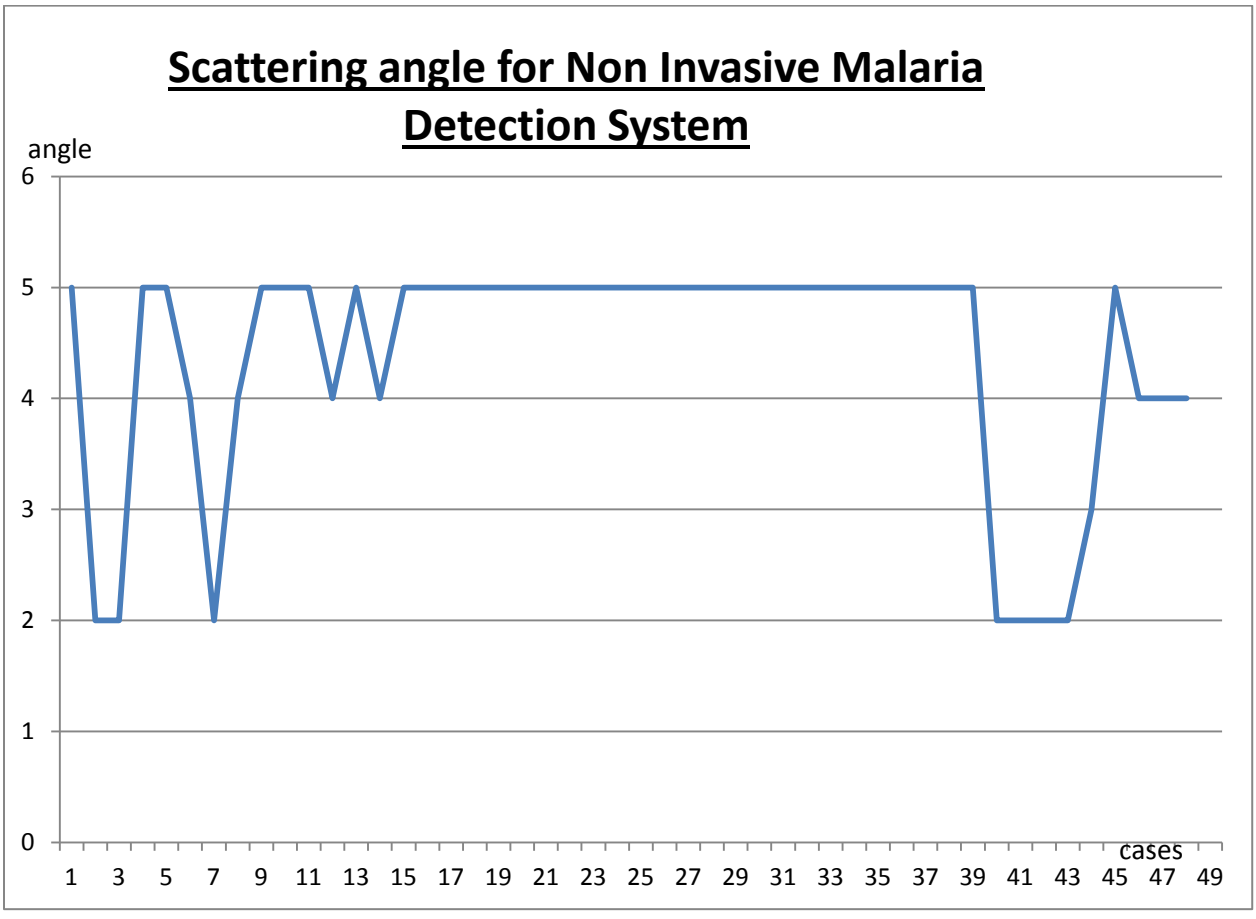

Figure (5.1): absorption values Vs scattering angle of non invasive malaria results

5.6 Verification result of the system

5.6.1 Predictive values

Now to verify our result we will find true positive value (TP), false positive value (FP), true negative value (TN), and false positive value (FN) from circuit measurements at table (5.5) to calculate sensitivity and specificity of the system.

Table (5.6): Predictive values (TP, TN, FP and FN) of the system

	Malarial	Non malarial	Total
Positive	30 (True Positive)	02 (False Positive)	32 $T_{Test\ Positive}$
Negative	17 (True Negative)	03 (False Negative)	20 $T_{Test\ Negative}$
	47 $T_{Malaria}$	05 $T_{Non\text{-}malaria}$	104 Total

$$\text{Prevalence of malaria} = \text{Total}_{\text{malaria}} \setminus \text{Total} * 100 \qquad (5.1)$$

$$\therefore \text{Prevalence of malaria} = 32 \setminus 104 * 100 = 30.76\%$$

The population used for the study influences the prevalence calculation.

5.6.2 Accuracy and sensitivity of the system

Sensitivity is the probability that a test will indicate 'malaria' among those with the malaria:

$$\text{Sensitivity} = \text{TP}/(\text{TP} + \text{FP}) \times 100 \quad (5.2)$$

$\therefore$ Sensitivity = 30/(30+02) × 100 = 93.7 %

Specificity is the fraction of those without malaria who will have a negative test result:

$$\text{Specificity} = \text{FN}/(\text{FN} + \text{TN}) \times 100 \quad (5.3)$$

$\therefore$ Specificity = 03/(03+17) × 100 = 15 %

Sensitivity and specificity are characteristics of the test. The population does not affect the results.

Positive Predictive Value is the chance that a person with a positive test truly has the disease, Negative Predictive Value is the probability of being in TP as compared to TN and they are calculating across the row as follows:

$$\text{Positive Predictive Value} = \text{TP}/(\text{TP} + \text{TN}) \times 100 \quad (5.4)$$

$\therefore$ Positive Predictive Value = 30/(30+17) × 100 = 63.8 %

$$\text{Negative Predictive Value} = \text{FN}/(\text{FN} + \text{FP}) \times 100 \quad (5.5)$$

$\therefore$ Negative Predictive Value = 03/(03+02) × 100 = 60 %

Accuracy

Accuracy is how close a measured value is to the actual (true) value.

$$\text{Accuracy} = \frac{\text{Number of correct samples}}{\text{Number of all samples}} * 100\% = \frac{47}{52} * 100 \quad (5.6)$$

$\therefore$ Accuracy = 90.38 %

5.7 Discussion

All volunteers reading was taken from the Germany Sudanese laboratory centre to test by prototype, with total readings (52) .Total of non malarial were Twenty readings divided into two section: true negative result (seventeen readings) give the scatter angle of value (2° to 4°) with absorption values from (450mV to 1248mV), as seen in table (5.5) and three false negative result with scatter angle of 5° and same absorption reading.

Another thirty-two malarial reading were divided to: true positive reading (thirty readings) were give scatter angle 5° with absorption value from (290 mV to 449 mV) and two false positive readings with same angles of negative samples).

We can say that scatter angle depend with absorption can identify malaria parasite non-invasively in the body with accuracy 90.38 %and sensitivity 93.7%, these are females results but unfortunately all reading for males are zero for scattering and absorption because of the wavelength of the source (650nm) and as we now from anatomy male tissue and muscle density is more than female. [25]

Chapter six

Conclusion and recommendations

6.1 Conclusion

The non-invasive techniques with their many unique properties are the result of

Developing in the medical field because it is more comfortable to the patient, help to reduce the errors and increase the accuracy of results.

The implemented design is a combination of LASER IR, magnet and embedded system which used to test (52) samples with (20) negative samples and (32) positive samples and conclude with satisfied results with test accuracy (90.38 %)and sensitivity (93.7 %).

This project used to diagnose malaria depending on the light interaction with human body to identify malaria parasite (hemezoin) with absorption and scattering angle values of the volunteers under investigation.

6.2 Recommendations

Depend on the result in the previous chapter, we recommend to:

1- Replacing the Laser IR source (HLM1230,650 nm,5mW) used in the circuit with Laser IR source (SPL CG81-2S,820 nm,5 mW) to reduce absorption light and increase the test accuracy and display male readings.

2- Adding three linear array photodiodes beside to accomplish another light interaction measurements (reflection and refraction) to understand their effect on the parasite.

3- Testing the other plasmodium species; thus the circuit becomes capable of distinguishing all types of malaria, with more volunteers.

References:

[1] Understanding malaria, U.S. Department of health and human services, National Institute of Allergy and Infectious Diseases. NIH Publication No. 07-7139. February 2007.

[2] www.who.int/world_malaria_report/en.

[3] www.malaria.com.

[4] T. Nishita, Y. Miyawaki, and E. Nakamae ," A shading model for atmospheric scattering considering luminous intensity distribution of light sources", In Proceedings of SIGGRAPH'87, pages 303–310. ACM Press, July 1987.

[5] Marcucci C, Madjdpour C and Spahn D .Allogeneic blood transfusions: benefit, Risks and clinical indications in countries with a low or high human development index. PMID 15339855. 2004.

[6] Htut, Y., Aye, K. H., Han, K. T., Kyaw, M. P., Shimono, K. and Okada, S. (2002), Feasibility and limitations of acridine orange fluorescence technique using a malaria diagnosis microscope in Mynamar, Acta Med. Okayama 46(5):219-222.

[7] Dave M. Newman, John Heptinstall,…etc ,(2008),A Magneto-Optic Route toward the In Vivo Diagnosis of Malaria:Preliminary Results and Preclinical Trial Data, University of Exeter, Exeter EX4 4QF, United Kingdom; Biophysical Journal Volume 95 July 2008 -3495/08/07/994/07.

[8] Aregawi, M., Cibulskis, R., Otten, M., Williams, R. and Otten, M. (2012), World Malaria Report 2012, WHO.

[9] Lema, O. E., Carter, J. Y., Nagelkerke, N., Wangai, M. W.,..etc Kitenge, P., G. (1999), "Comparison of five methods of malaria detection in the outpatient setting", American Journal of Tropical Medicine and Hygiene 60(2): 177-182.

[10] Storey, J. (2010), Basic Malaria Microscopy: Part 1. Learner's Guide, World Health Organization, Geneva.

[11] Makler, M. T., Ries, L. K., Ries, J., Horton, R. J. and Hinrichs, D. J. (1991), Detection of Plasmodium infection with fluorescent dye, benzothiocarborxypurine, American Journal of Tropical Medicine and Hygiene 44:11-16.

[12] Kawamoto, F. (1991) "Rapid diagnosis of malaria by fluorescence microscopy with light microscope and interference filter", Lancet 337:200-202.

[13] Htut, Y., Aye, K. H., Han, K. T., Kyaw, M. P., Shimono, K. and Okada, S. (2002), Feasibility and limitations of acridine orange fluorescence technique using a malaria diagnosis microscope in Mynamar, Acta Med. Okayama 46(5):219-222.

[14] Garcia, M., Kirimoama, S., Marlborough, D., Leafasia, J. and Rieckmann, K. H. (1996), "Immunochromatographic test for malaria diagnosis (Letter)", Lancet 347(9014):1549.

[15] Shiff, C. J., Minjas, J. N. and Premji, Z. (1994), "The Parasight®-F test: a simple rapid manual dipstick test to detect Plasmodium falciparum infection", Parasitology Today 10:494-495.

[16] Oliveira, D. A., Shi, Y. P. and Oloo, A. J. (1996), "Field evaluation of polymerase chain reaction based nonisotopic liquid hybridization assay for malaria diagnosis", Journal of Infectious Diseases 173:1284-1287.

[17] Tirasophon, W., Rajkulchai, P., …etc, (1994), "A highly sensitive, rapid and simple polymerase-chain-reaction method to detect human malaria (Plasmodium falciparum and Plasmodium vivax) in blood samples", American Journal of Tropical Medicine and Hygiene 51:308-313.

[18] Belisle, J. M., Costantino, S., Leimanis, M. L., Bellemare, M. J., Bohle, D. S., Georges, E, and Wiseman, P. W. (2007), "Sensitive detection of malaria infection by third harmonic generation imaging", Biophysical Journal: Biophysical Letters: L26-L28.

[19] Ong, C. W., Shen, Z. X., Ang, K. H., Kara, U. A. K. and Tang, S. H. (2002), "Raman microspectroscopy of normal erythrocytes and Plasmodium berghei-infected erythrocytes", Applied Spectroscopy 56:1126-1131.

[20] Grant, T. W., Leann, T., Samantha, D., Don, M. and Bayden, R. W. (2008), "Resonance Raman spectroscopy can detect structural changes in haemozoin (malaria pigment) following incubation with chloroquine in infected erythrocytes", FEBS Letters 582:1087-1092.

[21] Bremard, C., Girerd, J. J, Kowalewski, P., Merlin, J. C. and Moreau, S. (1993) "Spectroscopic investigations of malaria pigment", Applied Spectroscopy 47:1837-1842.

[22] Yulia, M. S., Patel, J. and Garcia-Rubio, L. H. (2010), "Interpretation of the ultraviolet-visible spectra of malaria parasite Plasmodium falciparum", Applied Optics 49 (2):180-188.

[23] Webster, G. T., Katherine, A.V., Egan, T. J., Tilley, T., Tobin, M. J., Bambery, K. R., McNaughton, D. and Wood, B. R. (2009), "Discriminating the intraerythrocytic lifecycle stages of the malaria parasite using synchrotron FT-IR microspectroscopy and an Artificial Neural Network", Anal Chem 81: 2516-2524.

[24] Linani Dickson Omucheni, M.Sc (Hons), University of Nairobi, Multispectral imaging of human blood media applied to malaria diagnostics, I56/72351/2012.

[25] Richard S.Snell, six edition, clinical anatomy for medical student book.

[26] Pieter van der Zee, "measurement and modeling of the optical properties of human tissue in the near infrared", Doctor of Philosophy (Ph.D.) of the University of London thesis, 1993.

[27] Cathy Chen, Shane Pryor, 2012, a Pulse Oximeter on an ATmega644 Microcontroller, IEEE journal

[28] Jamjoom, G. A. (1983) "Dark-field microscopy for detection of malaria in unstained blood films", Journal of Clinical Microbiology 17:717-721.

[29] Guillaume Poirier, 2003, "Human Skin Modelling and Rendering" thesis, Waterloo, Ontario, Canada, University of Waterloo.

[30] Dave M. Newman, Rapha el J. Matelon, M. Lesley Wears, and Luke B. Savage, "The In-Vivo Diagnosis of Malaria: Feasibility Study into a Magneto-optic Fingertip Probe Member", IEEE, May 2009, 10.1109/JSTQE.2009.2029068

[31] http://www.nature.com/nbt/journal/v20/n11/images/nbt11021098F1.gif

[32]http://www.chaffey.edu/mathandscience/tr/categories/photos/plasmodim.falciparum

[33] http://www.dpd.cdc.gov/dpdx/images/ParasiteImages/M-R/Malaria/vivax

[34] http://www.dpd.cdc.gov/dpdx/images/ParasiteImages/M-R/Malaria/malariae

[35] http://www.dpd.cdc.gov/dpdx/images/ParasiteImages/M-R/Malaria/ovale

[36] http://www.physicsclassroom.com/class/refln/Lesson-1/snell-law

[37] https://www.google.com/search?q= snell-law +equation&newwindow

[38] http://scienceworld.wolfram.com/physics/absorption+scattering.html

[39]Guillaume Poirier, "Human Skin Modelling and Rendering" thesis ,Waterloo, Ontario, Canada, University of Waterloo, 2003.

[40] R.V. Klassen," Modeling the effect of the atmosphere on light",ACM Transactions on Graphics, 6(3):215–237, July 1987.